Contents

List of Figures

1 APPENDIX I —Oscillator Theory, Hamilton's Style

Our discussion begins with a consideration of the simple harmonic oscillator (SHO) without drive. We are most accustomed to its representation (equation of motion) as a 2nd order, linear, ordinary differential equation:

$$d^2x/dt^2 + 2\beta dx/dt + \omega_0^2 x = 0 \tag{1}$$

which is alternatively written as

$$\ddot{x} + 2\beta\dot{x} + \omega_0^2 x = 0 \tag{2}$$

(Newton was the first to use the dots over a variable to indicate time derivatives.) Because it is linear, the solution is straightforward, even in the inhomogeneous case (non-zero right hand side). The most elegant analysis is one involving the transform mathematics given to us by Laplace, an analysis that is possible because the equation is linear. Interestingly (in spite of his greatness) Laplace was seriously wrong on one account. He insisted that the future of any system could be predicted, at any time, with any accuracy—assuming that the present state could be adequately specified. Of course the "butterfly effect" of chaos demonstrates that this is not true for complex systems. One indisputable consequence of this effect is that weather, for example, will never be amenable to long term accurate predictions.

There's a curious historical development regarding the Laplace transform. Physicists are operationally more knowledgeable of the Fourier transform than the Laplace transform, whereas the opposite is true of most engineers. Many physicists are prone to believing that the Fourier transform is the more general of the two, when in fact the opposite is true. None of this is particularly important for the treatment of complex systems, since the nonlinearity necessary for their existence disallows superposition and thus the use of transform theory in the construction of a solution. It should be noted, however, that the fast Fourier transform (FFT) has become an important tool for the study of chaos. Periodic motion is readily recognized by its spectral character (well defined lines produced by the FFT), whereas chaotic motion gives broad features generally devoid of well defined lines (although the drive of a chaotic system will usually show up in the power spectrum as a distinct line.) For one unfamiliar with the Fourier transform, it may be convenient to consider its graphical treatment involving vectors in the complex plane (R. Peters, "Fourier transform construction using vector graphics", Amer. J. Phys. 60 (5), 439, 1992).

When it comes to nonlinear systems, analytic methods for their treatment are still in a stage of relative infancy. There are certain nearly universal characteristics that facilitate the "big picture". For example, the work of Feigenbaum showed that all systems with a quadratic potential should have features similar to those of the most fundamental of iterative equations–the logistic (or quadratic) map

$$x_{n+1} = c\, x_n\, (1 - x_n) \tag{3}$$

where c is a constant.

When the pendulum demonstrates a phase space "loop-the-loop" 1/2 subharmonic response, it is in some respects showing behavior similar to the logistic map following the first bifurcation in its period doubling route to chaos. (Subharmonics are not possible in linear systems.) Unlike the pendulum, where the steady state response for this case is at 1/2 the drive frequency, the logistic map, being discontinuous, generates a sequence in which, for this case, x-values repeat every two iterations of the map (in the steady state). Additionally, the logistic map involves only one variable (1-dimensional) whereas the pendulum with damping and drive involves 3 variables. Nevertheless, there are some similarities and a greater appreciation of such can be realized by considering the numerical solution to the pendulum in which the equation of motion is written in terms of finite difference expressions. In principle, the pendulum can be solved by integrating the 2nd order equation: first of the angular acceleration to get velocity, and second of the angular velocity to get position. In practice, the accuracy of the final result is much better if one works with an equivalent pair of first order differential equations rather than the single second order one. The manner in which this is done will now be described.

The equation of motion for the simple non-driven pendulum without damping is as follows:

$$\ddot{\theta} + (g/L)sin\theta = 0 \tag{4}$$

The nonlinear term is that of $sin\theta$, which can be replaced with θ when the amplitude of the motion is small; since it is the first term in the McClaurin series expansion. It is well known that, in general, a 2nd order differential equation can be replaced with a pair of first order ones. The techniques of mathematics whereby this can be accomplished need not be considered by physicists; rather the natural approach is to use Hamilton's canonical equations. In the days when Goldstein's famous textbook on mechanics was written, it was true that the primary reason for studying the Hamiltonian in classical dynamics was as a "stepping stone" into quantum mechanics. With the advent of chaos, this is no longer the case. The canonical equations of Hamilton are the simplest way to obtain the desired pair of first order equations. His approach is based in Lagrange's method. Consider, for example, the physical pendulum.

The Lagrangian, Λ, is given by

$$\Lambda = T - V, \quad T = \frac{1}{2}I\,\dot{\theta}^2 \tag{5}$$

where

$$V = mgL(1 - cos\theta) \rightarrow -mgL\,cos\theta \tag{6}$$

In turn, the equation of motion becomes

$$d/dt(\partial\Lambda/\partial\dot{q}) = \partial\Lambda/\partial q \quad , \quad q = \theta \tag{7}$$

Therefore,

$$\Lambda = \frac{1}{2}I\,\dot{\theta}^2 + mgL\,cos\theta \tag{8}$$

and thus

$$p = \partial\Lambda/\partial\dot{q} \rightarrow I\,\dot{\theta} \tag{9}$$

$$\partial\Lambda/\partial q = -mgL\,sin\theta \tag{10}$$

so that the final equation of motion is

$$I\ddot{\theta} + mgL\,sin\theta = 0 \tag{11}$$

or, alternatively,

$$\ddot{\theta} + \omega_0^2\,sin\theta = 0 \tag{12}$$

The Hamiltonian method uses the Lagrangian in the following way.
The Hamiltonian is given by:

$$H(p,q) = \sum p_i\dot{q}_i - \Lambda = 2T - \Lambda = T + V = E \tag{13}$$

For the pendulum

$$E = \frac{1}{2}I\,\dot{\theta}^2 - mgL\,cos\theta , \quad p = I\,\dot{\theta} \tag{14}$$

$$H = p^2/(2I) - mgL\,cosq \tag{15}$$

$$\partial H/\partial p = \dot{q} \quad , \quad \partial H/\partial q = -\dot{p} \tag{16}$$

4

or

$$p/I \; = \; \dot{q} \quad , \quad mgL \; sin \; q \; = \; -\dot{p} \tag{17}$$

which is the desired pair of 1st order differential equations. Also this yields

$$I\ddot{q} \; + \; mgL \; sin \; q \; = \; 0 \tag{18}$$

as before.

Let's reiterate this Hamiltonian methodology for the simple pendulum. To obtain the Hamiltonian from the energy expression, the kinetic energy must be written in terms of the momentum conjugate to θ . For simple systems, this can often be recognized by inspection. In general, and for more complicated systems, the conjugate momentum is, by definition, the partial derivative of the Lagrangian (T - V) with respect to the time differentiated variable of interest. In the case of our simple pendulum,

as opposed to the so-called physical pendulum:

$$E \; = \; \frac{1}{2}m\dot{\theta}^2 L^2 - mgLcos\theta \tag{19}$$

This gives us the Hamiltonian

$$H \; = \; \frac{p^2}{2mL^2} \; - \; mgLcos\theta \tag{20}$$

Note that $\dot{\theta}$ must be expressed in terms of p before $H \; = \; H(p,q)$. The canonical ("God-given") equations which use this Hamiltonian are as follows:

$$\frac{\partial H}{\partial p} \; = \; \dot{\theta} \; = \; \frac{p}{mL^2} \tag{21}$$

$$\frac{\partial H}{\partial \theta} \; = \; -\dot{p} \; = \; mgLsin\theta \tag{22}$$

The simple pendulum is not capable of chaos, since motion "over-the-top" (past vertical) is not allowed with a weightless (flexible) support wire. Thus the physical pendulum must be considered, for which the equation of motion (non-driven) is as follows:

$$I\ddot{\theta} + c\dot{\theta} + mgL \; sin\theta \; = 0 \tag{23}$$

where the loss has been accommodated, to a useful first approximation for many cases, by a single term (the one containing c in Eq. 23). An unconventional Hamiltonian description can be written, which includes the external drive torque, $\tau(t)$ and a damping term, $c \; p$.

$$\frac{\partial H}{\partial \theta} \; = \; mgL \; sin\theta \; + \; cp \; = \; -\dot{p} \; + \; \tau(t) \tag{24}$$

$$\frac{\partial H}{\partial p} \; = \; \dot{\theta} \; = \; \frac{p}{I} \tag{25}$$

To convert these into a finite difference form, for Cromer-Euler integration, the definition of the time derivative is employed, to give:

$$\frac{\Delta p}{\Delta t} \; = \; \tau(t) - mgL \; sin\theta - cp \tag{26}$$

$$\frac{\Delta \theta}{\Delta t} \; = \; p \; / \; I \tag{27}$$

1.1 Phase Space

The canonical variables of Eq. (24) and (25) are θ and the momentum conjugate to it, p. Notice that the equations of motion are of the form

$$
\begin{aligned}
\dot{x}_1 &= F_1(x_1, x_2, x_3, ...) \\
\dot{x}_2 &= F_2(x_1, x_2, x_3, ...) \\
\dot{x}_3 &= F_3(x_1, x_2, x_3, ...)
\end{aligned}
\tag{28}
$$

This general set of expressions is a useful means for determining whether the system is conservative or dissipative [as described by Baker and Gollub (see ref. (5) of Appendix II)]. The derivative terms (velocities in phase space) are associated with flows in the space. The flux from a small region is given by

$$
\text{Flux} = \int_S \mathbf{F} \cdot \mathbf{n} \, \text{dS}
\tag{29}
$$

where $\mathbf{n}$ is the unit normal vector to the surface, S. Phase area will be preserved if the flux is zero. Conversely, a negative flux indicates that there is dissipation. Using the divergence theorem, which converts a surface integral into a volume integral, Eq. (29) yields

$$
\int_S \mathbf{F} \cdot \mathbf{n} \, \text{dS} \rightarrow \int_V \nabla \cdot \mathbf{F} \, \text{dV}
\tag{30}
$$

To determine if there's dissipation, one need only determine if $\nabla \cdot \mathbf{F}$ is negative; i.e., check the sign of

$$
\frac{\partial F_1}{\partial x_1} + \frac{\partial F_2}{\partial x_2} + \frac{\partial F_3}{\partial x_3} + \ldots
\tag{31}
$$

Keep in mind, according to Hamilton's theory, that x_1, x_2, x_3, ... are independent variables.

Let's take the case of the pendulum that was just treated. x_1 corresponds to θ and x_2 corresponds to p. In turn, $F_1 = p/I$ and $F_2 = -mgL \sin\theta - cp + \tau(t)$. Even though $p = I\dot{\theta}$, in evaluating the partial derivatives for the divergence, they are treated as independent variables. Thus we come up with the result that

$$
\nabla \cdot \mathbf{F} = -c
\tag{32}
$$

As expected, the dissipation is associated with the constant which we earlier said determines the damping of the pendulum.
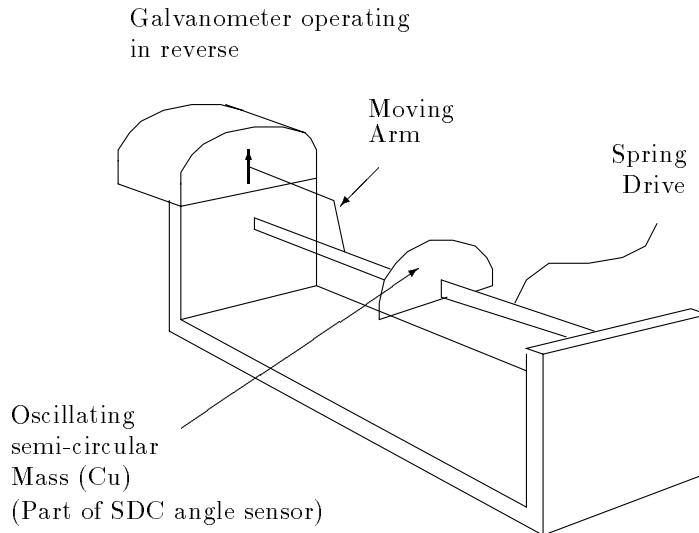
Figure 1: Torsion-Gravity Pendulum.

2   APPENDIX II —Chaotic Torsion-Gravity Pendulum

When operating in a chaotic manner, the driven simple pendulum undergoes large angle changes. This is also true of the more complex double pendulum [1]; however, a pendulum which is influenced by torsion can display chaos at both small as well as large amplitudes [2]. Unlike the simple pendulum, this one can be configured to have two wells, like a buckled beam or Duffing type oscillator. The present configuration is one in which a mass is fixed at the center of a horizontal metal ribbon which is secured at both ends to a rigid stand as shown in Fig. 1.

If the acceleration of gravity, g , could be "turned off", the equilibrium position of the mass (zero displacement) would be above the ribbon. When the mass is displaced from equilibrium, the system oscillates with a motion that is determined by the torques from gravity and torsion acting in opposition. In one study of this pendulum, the oscillating mass was part of an angle sensor, being a planar copper semi-circle. The drive source (essentially a loudspeaker—Pasco string driver) was variable in both amplitude and frequency. It was coupled to the ribbon using a weak "leaf" spring. Additionally, a galvanometer operating in "reverse" was mechanically linked to the ribbon with a wire. Motion of the needle gave an output voltage proportional to the velocity. Output from the position and velocity sensors was coupled into the the x and y inputs respectively of a recorder.

2.1   Apparatus

The torsion member of the pendulum was a carbon steel ribbon 0.2 mm thick; whose length was 60 cm, and whose width was 6 mm. On each end of the ribbon are screws (brazed in place), which pass through holes drilled in a pair of rigid vertical end plates. Using two nuts per screw (one on the inside and the other on the outside of the end plate, both the tension in the ribbon and the equilibrium position of the oscillating mass could be adjusted. Cut from copper sheet, 0.5 mm thick with a diameter of 10 cm, the oscillating mass was soldered to the ribbon at its center. Its position was measured with a symmetric differential capacitive (SDC) angle sensor [3]. Each of the static plates of the angle sensor had a 12 mm hole drilled in the center to pass the ribbon. Because there is no mechanical contact with the moving parts, this sensor is virtually non-perturbing. The range of operation of a single SDC angle sensor of this type is $\pm\pi/2$, which proved to be more than adequate for the work that is being described.

To measure the angular velocity of the pendulum, a thin (stiff) metal arm bent in the shape of an "L" was soldered to the ribbon at a point 5 cm from the mass. This arm was connected, in turn, to

the needle of the galvanometer; it was adjusted so that zero on the scale corresponded to zero of the pendulum. The use of this velocity detector was deemed preferable to operating with only the angle sensor and differentiating, since differentiation can destroy signal to noise ratios in the absence of a good filter, which was not available.

The drive was provided with a Hewlett Packard function generator connected to the loudspeaker through a power amplifier. A sine signal in the range $0.1 \rightarrow 0.6$ Hz was used. An arm protruding from the center of the speaker was attached by means of a thin (weak) "wavy leaf" spring to the top edge of the ribbon. In this way, horizontal movements of the speaker cone produced torques on the ribbon. Thus the drive could be transmitted to the pendulum while still allowing the ribbon to twist in relative freedom.

2.2 Analysis

In this first treatment, the damping and external drive will be ignored. Additionally the torsion constant of the ribbon will be set to unity, resulting in a dimensionless form. This procedure is common in the literature dealing with chaotic systems. It will readily allow a comparison of the present system with the Duffing oscillator. Later, the full equations will be provided.

The potential energy due to fiber twist can be accurately described by a parabola. The potential energy of the oscillating mass due to gravity is a cosine function. Combining the two gives

$$V(\theta) \;=\; \frac{1}{2}\,\theta^2 + b\,\cos\,\theta \tag{33}$$

Taking the derivative yields the torque

$$\tau(\theta) \;=\; -\,\theta + b\,\sin\,\theta \tag{34}$$

The parameter b determines the depth and the separation of the two wells. The value of b was determined by setting τ to zero and θ_{eq} equal to the angle displaced when the mass is at rest in a well. An angle of $0.366\ rad$ gives $b = 1.023$. Finally, with no drive and no dissipation, it can be seen that the equation of motion is

$$\ddot{\theta} \;+\; \theta \;-\; b\,\sin\,\theta \;=\; 0 \tag{35}$$

As noted before, the Hamiltoniantechnique is a powerful one for obtaining the equations of motion. It is thus used here to obtain the same result as Eq. (35).

For the torsion-gravity pendulum, there are two parts to the potential energy, the $\frac{1}{2}k\theta^2$ from the elastic ribbon and also the part from gravity (since the zero is vertically overhead),

$$V_g(\theta) \;=\; mgL(\cos\theta \;-\; 1) \rightarrow mgL\,\cos\theta \tag{36}$$

The Hamiltonian is given by

$$H \;=\; p^2/(2I) \;+\; \frac{1}{2}k\theta^2 \;+\; mgL\,\cos\theta \tag{37}$$

which gives the canonical equations

$$\partial H/\partial p \;=\; p/I \;=\; \dot{\theta} \tag{38}$$

$$\partial H/\partial \theta \;=\; k\theta \;-\; mgL\,\sin\,\theta \;=\; -\dot{p} \tag{39}$$

The equations are made dimensionaless by setting $p \;=\; \dot{\theta}$, $\dot{p} \;=\; b\,\sin\,\theta \;-\; \theta$
giving the equation of motion

$$\ddot{\theta} \;+\; \theta \;-\; b\,\sin\,\theta \;=\; 0 \tag{40}$$

For comparisons against early experiments, the value of b was restricted to values slightly greater than 1. The model is rich in diversity, however, when b can take on a wide range. In the limit $b \rightarrow 0$

8

(spring dominant), it becomes the simple harmonic oscillator, the paradigm of linear physics. For $b \gg 1$ (gravity dominant), it becomes the pendulum, the paradigm of nonlinear physics, as first recognized by B. V. Chirikov.

Eqns. (38) and (39) were used to obtain the following map:

$$p_{n+1} = p_n + b \, sin \, \theta_n - \theta_n \tag{41}$$

$$\theta_{n+1} = \theta_n + p_{n+1} \tag{42}$$

This pair of equations is similar to the Chirikov map except that $c \to -b$ and $-\theta_n$ has been added. Some of its fractal properties for $b > 1.5$ have been noted [4].

The equation of motion was linearized for small oscillations about an equilibrium. Setting $\eta = \theta - \theta_{eq}$ and substituting into Eq.(39) yields

$$\ddot{\eta} + \eta + \theta_{eq} - b \, sin(\eta + \theta_{eq}) = 0 \tag{43}$$

Expanding $sin(\eta + \theta_{eq})$ yields

$$\ddot{\eta} + \eta + \theta_{eq} - b \, (sin \, \eta \, cos \, \theta_{eq} + sin \, \theta_{eq} \, cos \, \eta) = 0 \tag{44}$$

Using the small angle expressions for $sin \, \eta$ and $cos \, \eta$ and $\theta_{eq} = b \, sin \, \theta_{eq}$ gives

$$\ddot{\eta} + \eta \, (1 - b \, cos \, \theta_{eq}) = 0 \tag{45}$$

Thus the angular frequency of this idealized system at small amplitudes about either equilibrium point is

$$\omega_0 = \sqrt{1 - b \, cos \, \theta_{eq}} \tag{46}$$

2.3 To compare with Experiment

The full equation of motion for the pendulum, including a viscous damping term, $c \, \dot{\theta}$, and the external driving torque, $\tau \, (t)$ is:

$$I \, \ddot{\theta} + c \, \dot{\theta} + k \, \theta - mgL \, sin \, \theta = \tau \, (t) \tag{47}$$

where I is the moment of inertia of the rotating member, k is the ribbon torque constant, g is the acceleration of gravity, m is the mass of the rotating member, and L is the distance of its center of mass from the ribbon. To compare with Eq.(46), we set $\tau = 0$, and as before show that small oscillations about an equilibrium (for small c) are at the angular frequency

$$\omega_{0,actual} = \sqrt{\frac{k}{I}} \, \sqrt{1 - \frac{mgL}{k} \, cos \, \theta_{eq}} \tag{48}$$

The steps which yielded Eq.(45) (dimensionless) is tantamount to scaling the time; therefore ω_0 is not truly a frequency. Rather, it is proportional to the frequency, and the proportionality constant is seen to be $\sqrt{\frac{k}{I}}$. Additionally, from Eq.(48) it is seen that $b = mgL \, / \, k$. Moreover, the equilibrium point is obtained by equating the magnitudes of the oppositely directed torques of gravity and torsion to give $\theta_{eq} = \frac{mgL}{k} \, sin \, \theta_{eq}$.

These results were used to compare theory and experiment in a variety of cases that are reported in the paper: R. Peters, "Chaotic mechanical oscillator based on torsion and gravity in opposition", to be published in the American Journal of Physics.

2.4 Computer Simulation

The experimental system contains three independent dynamical variables when the drive is included. It is best described in terms of three coupled 1st order differential equations, as follows:

$$I \, \frac{d}{dt} \, \omega = - k \, \theta + mgL \, sin \, \theta - c \, \omega + A \, cos \, \phi \tag{49}$$

$$\frac{d}{dt} \, \theta = \omega \tag{50}$$

$$\frac{d}{dt} \, \phi = \omega_d \tag{51}$$

Thus it meets the minimum condition for chaotic motion as indicated on p. 3 of Baker and Gollub [5]. It should be noted that chaotic systems of the type first studied by Chirikov and coworkers can be ones with fewer than three variables. In Moon's book [6], these conservative (non-dissipative) cases are referred to as Hamiltonian systems (p.19). A classic example of chaos of this type is the Henon-Heile problem (c.f., p. 39 of [7]). Interestingly, the best way to obtain the 1st order differential equations for the system is by using Hamilton's techniques. We once thought that the primary reason for Hamilton's canonical equations in classical dynamics was as a "stepping stone" into quantum mechanics. Now it is recognized that they provide a better way to do computational physics. In particular, if one integrates a 2nd order equation twice, rather than a coupled 1st order set once; then the errors are worse.

Integration of all the equations of motion was done using the Cromer-Euler algorithm, also called the Last Point Approximation [8]. The program proved to be reasonably accurate, versatile, and easy to use.

2.5 Hysteresis

One question that has arisen in relationship to this work deals with hysteresis in nonlinear systems. One form of the Duffing oscillator is well known for its amplitude jumps around a hysteresis loop. This well known "hardened" oscillator case [9] (c.f., p.148) is one for which α is negative—the opposite sign to the present case. It is not known whether the Duffing oscillator which the present pendulum approximates for small b is also capable of hysteresis jumps. Jumps in the driven rigid planar pendulum [10] have been observed (overwhelmingly downward). As there, the existence/properties of hysteresis should be readily answerable via computer modelling by modifying TABLE I. The modification is one in which the frequency of the drive would be altered during execution, rather than being fixed as for the present cases. If amplitude jumps should occur (at critical frequencies), the magnitude of a jump would be the difference between the steady state amplitudes of the motion before and after the event. It is important in such an investigation that the rate of drive frequency alteration be slow compared with transient settling times.

TABLE I. Simulation of the torsion-gravity pendulum

```
    REM Shift F5 to run, Ctrl Break to exit
CLS
PRINT "which frequency? (.16 is chaotic, .12 a limit cycle)"
INPUT df
PRINT "Which display? ('P' for Poincare, [return] for phase space trajectories]"
INPUT dtype$
CLS
PRINT dtype$
SCREEN 9
REM define resolution for vga graphics
LINE (275, 290)-(325, 290)
LINE (275, 250)-(275, 290)
LOCATE 21, 43: PRINT "q"
LOCATE 19, 36: PRINT "p"
redo:
LOCATE 1, 1
IF dtype$ = "p" THEN PRINT "TORSION-GRAVITY PENDULUM-POINCARE' SECTION"
IF dtype$ <> "p" THEN PRINT "TORSION-GRAVITY PENDULUM-PHASE SPACE"
LOCATE 23, 10
PRINT "press 'c' to clear (to look for steady state), 'x' to exit"
REM color can be removed if desired
COLOR 15, 4
REM Set numerical values for constants
tpi = 3.1416 * 2
```

```
da = .0018
b = 1.023: c = .02
dt = tpi / 20
LOCATE 3, 1: PRINT "b ="; b: PRINT "drv. freq. ="; df: PRINT "drv. ampl. ="; da
PRINT "damping ="; c
REM set 'position' & 'scaling' of the graphics output
VIEW (0, 0)-(600, 349)
WINDOW (-.4, -.4)-(.4, .4)
REM start the main program
start:
t = t + dt
REM update the angular velocity
dp = -th + b * SIN(th) - c * p5 + da * COS(df * t)
p5 = p5 + dp * dt
REM update the angle
dth = p5
th = th + dth * dt
REM generate a point in the user selected display
REM clear screen if "c" pressed
IF INKEY$ = "c" THEN CLS : GOTO redo
IF dtype$ <> "p" THEN GOTO 112
REM create a Poincare section: place a pixel at (x,y) once per drive cycle
q = COS(df * t)
IF ABS(q - 1) < .0005 THEN PSET (.5 * th, 4 * p5)
GOTO start
112
REM create a phase plot
LINE (.5 * pth, 2.5 * pp5)-(.5 * th, 2.5 * p5)
pth = th
pp5 = p5
GOTO start
END
```

The TABLE I routine has been part of the previously mentioned Physics 5300 course on chaos and complexity; it proved very popular with the students, when coupled with other software [11]. Many of these are part of the "TELAWARE" General Simulations menu (GSM). For those who would like to improve their knowledge of chaos, these software packages are highly recommended. They include: Poincare' sections, time history plots, and fast Fourier transforms (FFT) to generate power spectra. Using a 486 Intel based PC computer, Poincare' sections involving thousands of points can be generated in a matter of minutes. To generate such a section, pixels are recorded only at the start of every drive cycle. For example in TABLE I, a short time window for which the cosine term is in the vicinity of unity regulates pixel recording. This is only one of an infinity of possible fractals, depending on the phasing.

Of the routines used for chaos studies, the Poincare' section is far and away the best single indicator of chaos; which is a tribute to the French mathematician for whom the graph is named, and who lived before the age of chaos. Sensitive dependence on initial conditions is the least useful; in fact, cases used to demonstrate it may not themselves be chaotic at all. They simply suggest that the potential for chaos exists, for different parameter choices. The power spectrum is also rather limited. Many believe that chaos implies spectral features without any "lines"; however, there can be spectral lines present. For example, periodicity associated with the drive is usually evident in the autocorrelation of the time record.
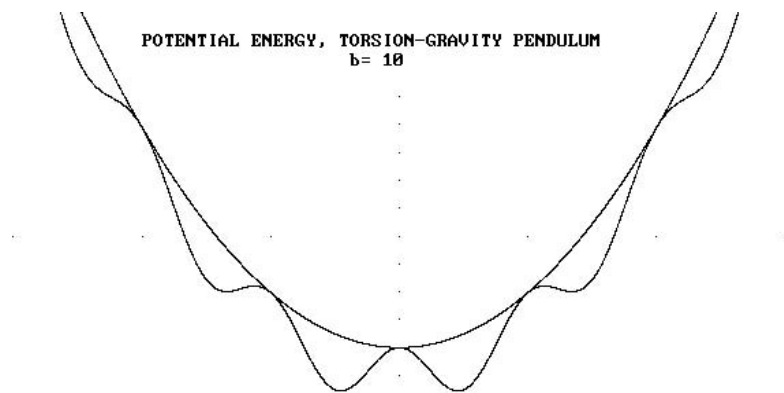
```
POTENTIAL ENERGY, TORSION-GRAVITY PENDULUM
                    b= 10
```

Figure 2: Torsion-gravity pendulum potential with large b.

2.5.1 Large b results

When $b \gg 1$ the potential energy of the pendulum takes on the character of a "modulated" parabola, as shown in Fig. 2. For reference purposes, the harmonic potential is also indicated. This system is especially interesting because of its strong "trapping" tendencies. It may be a paradigm for the nonlinearity of otherwise Hookean systems, when the displacements are very small. We are accustomed to believing that nonlinearity (a necessary but not sufficient condition for chaos) occurs only for large motions of a mechanical system. Studies that were a part of [4] demonstrated that mechanical system oscillations are also quite nonlinear in the mesoscopic realm. Additionally, they display numerous kinds of cooperative behavior [12]. The "atomic musical chairs" that are a part of anelasticity, are responsible for "modulation" of the otherwise harmonic potential. Thus the present system may be a useful beginning point for understanding mesoanelasticity. More information on these topics is found in Appendix V.

References

[1] R. B. Levien and S. M. Tan, "Double pendulum: An experiment in chaos", Am. J. Phys. *61*, 1038-1044 (1993).

[2] R. D. Peters, "Mechanically adjustable balance and sensitive tilt meter", Meas. Sci. Technol. *1*, 1131-1135 (1990).

[3] R. D. Peters, "Capacitive angle sensor with infinite range", Rev. Sci. Instrum *64*, 810-813 (1993). (Note: For the present work a single unit with $\pm\pi/2$ range was used, rather than the dual unit system described in the referenced paper.)

[4] R. D. Peters, "Experimental evidence for a new frontier— mesoanelastic complexity", Proc. Non-linear Phenomena in Complex Systems, Belarus (1994).

[5] G. Baker and J. Gollub, *Chaotic Dynamics, an Introduction*, Cambridge University Press (1990).

[6] F. Moon, *Chaotic and Fractal Dynamics, An introduction for Applied Scientists and Engineers*, Wiley, New York (1992).

[7] S. Koonin, *Computational Physics*, Benjamin Cummings, Menlo Park, CA (1986).

[8] A. Cromer, "Stable solutions using the Euler approximation", Am. J. Phys. *49*, 455-457 (1981).

[9] J. Marion and S. Thornton, *Classical Dynamics of Particles and Systems*, 3rd ed., Harcourt Brace Jovanovich, San Diego (1988).

[10] R. Peters, "Resonance response of a moderately driven rigid planar pendulum", to be published in the Amer. J. Phys. (1994).

[11] W. Press, B. Flannery, S. Tuikolsky, and W. Vetterling, *Numerical Recipes, the art of Scientific Computing*, pp. 381-453, Cambridge University Press (1986).

[12] R. Peters, "Cooperative Phenomena of Mesodynamics", Proc. Conf. on Synergetics, Belarus (1994).

3 APPENDIX III—Kalman Filtering

It was mentioned in Section 5.4 that Kalman filtering is used in the U. S. Army's AH-1S Bell Air Cobra helicopter. In that system, developed in the 1970's, several observables were factored into the optimal estimates that were part of the fire control system. They included range to target, aircraft ground velocity and air velocity, and the pointing angles and associated rates of the tow missile sighting unit (TSU). Respectively, these were measured with a laser, radar and Bernoulli based instruments, and gimbal mounted instruments of the TSU. As with most systems of this type, there can be complex inter-relationships among various subsystems. For example, the first attempt at pointing the chain gun was a disaster, because the direction cosines of the barrel were computed absolutely. This proved to be an unacceptable solution because of rounding errors in the onboard computer. It had been realized sometime earlier by a minority of physicist employees (primarily Walt Yancey) that the smart solution would be one based on a perturbation of the gun direction from the TSU line of sight. Anticipating problems with the planned approach, this backup method was already in place and readily implemented when the physicists'predictions proved true.

Fortunately, even in a complex system, such as the AH-1S, linear approximations are acceptable under properly recognized constraints. If this were not the case, then Kalman filtering techniques would be useless. In the cobra's case, theoretical relationships among the variables mentioned were used to construct the filter. These were kinematic ones, relating, for example, the range to target and angle rates of the line of sight. Of course there are various errors, primarily random, which figure into the problem, an example being the small deviations of the target image about the gunner's crosshairs. Because the parameters are digitized, there are always the rounding errors of this process. The Kalman filter was designed to "smooth" the variables in an optimum sense. As was mentioned in section 5.4, the pendulum is a prototypical example of such filtering, and is now presented.

3.1 Simple Pendulum

The foundation for the filter are found in section 5.4 (equations 12 - 13). The filter requires a set of coupled first order differential equations in the state variables. For the pendulum, the state variables are T and $\dot{T}$. That which follows is valid to the extent that $\ddot{T} = -2\dot{T}/\Delta$. The characteristic of the physical system that is most likely to invalidate this assumption is the decay law. Nelson and Olsson [1] show that the viscous contributors to the damping of a pendulum derive from two parts: (i) wire, and (ii) bob—and the different Reynold's number for the two give rise to a more complicated decay law than a simple exponential. In particular, their work suggests a decay as follows

$$\theta_0 = \frac{\alpha\theta_{00}e^{-\alpha t}}{\beta\theta_{00}(1 - e^{-\alpha t}) + \alpha} \tag{52}$$

In other work [2], Eq. (52) was compared with the single exponential by setting β to zero and assigning α a new value. The new α was obtained by applying linear regression to the logarithm of the amplitudes generated from (52). Using coefficients representative of the pendulum studied and time intervals up to 10 minutes, the single exponential expression never differed from (52) enough to generate period errors larger than $4 \mu s$. Additionally, the correlation coefficient was less than 0.0004. Since actual decay-constant measurements (also by log regression) never correlated this well, it was decided that the single exponential approximation was valid, for measurement times less than 10 minutes.

3.2 State Equations

The measurement and the estimate of period differ because of system noise. The variance of the measurement error will be denoted by V_M. Two coupled first order differential equations in the period and period rate estimates describe the system as approximated. These equations and the associated variance equations following them derive from the theory provided in [3].

$$\frac{dT}{dt} = \dot{T} + \frac{V_{11}(t)(T_M - T)}{V_M \quad min} \tag{53}$$

$$\frac{d\dot{T}}{dt} = -\frac{2\dot{T}}{\Delta} + \frac{V_{12}(t)(T_M - T)}{V_M \quad min} \tag{54}$$

Here T_M is the measured period. In the following variance equations, the subscript 1 is associated with T and the subscript 2 with $\dot{T}$.

$$\frac{V_{11}}{dt} = 2\,V_{12} - \frac{V_{11}^2}{V_M \quad min} \tag{55}$$

$$\frac{V_{22}}{dt} = -\frac{V_{12}^2}{V_M \quad min} - 4\frac{V_{22}}{\Delta} \tag{56}$$

$$\frac{V_{12}}{dt} = V_{22} - 2\frac{V_{12}}{\Delta} - \frac{V_{11}V_{12}}{V_M \quad min} \tag{57}$$

The coupled set, (55)-(57), are numerically integrated as the measurement is introduced at each update point. In [2], the measurements were five-period averages (approximately 11.9 s) with a one-period deadtime (2.38 s) during which the counter (a Hewlett-Packard) was reset. Thus the update time interval (integration step size) was six pendulum periods, or roughly 0.238 minutes. Several integration techniques were tried, including Runge Kutta. It was found that the simple Euler-Cromer scheme worked well, giving numerical errors an order of magnitude smaller than the estimation uncertainties.

3.3   Initial Conditions

Past experiments have sometimes attempted to improve estimation accuracy by going to very small amplitudes. For example, a typical value in the measurements of [4] was about 5 mrad. The stochastic measurement errors, however, should be an inverse function of the signal-to-noise ratio; i.e, the measurement error should increase as the ideal (noise free) amplitude decreases. This was shown to be true in the experiments of [2]. Also shown there are graphs (figures 7-9) of how the variances decay (almost exponentially) with time. The standard deviation of the period was found to be $3.5\ \mu s$, for an average over five groups of measurements made at different times. It is now known that this data was influenced largely by atmospheric pressure measurements. It would be worthwhile repeating them with corrections for barometric change. With such corrections, it might be possible to once again make the pendulum a viable contender for accurate estimates of the local acceleration of gravity.

3.4   Conclusions

It was noted in [2] that physicists have not, for the most part, taken advantage of a powerful estimation tool, even though it is one that is rooted in Hamiltonian mechanics [5]. This tool has tremendous potential in many areas of experimental research. The benefit results (in a qualitative sense) because the technique is an extension of the "static" linear regression problem to its more general dynamic form. The nomenclature is not common to physicists, however, so a time investment for education is required. As noted in [2], that investment has the potential for handsome dividends.

REFERENCES
(1) R. A. Nelson and M. G. Olsson, *Amer. J. Phys.* 54 (2), 112 (1986).
(2) R. D. Peters, *Appl Math. and Comp.* 28, 179 (1988).
(3) A. Gelb (Ed.) *Applied Optimal Estimation* MIT Press, Cambridge,
Mass., 102 (1984).
(4) P. R. Heyl and G. S. Cook, *J. Res. Nat. Bur. Standards* 17, 805 (1936).
(5) M. Athans and E. Tse, *IEEE Trans. Automat. Control*, 690 (1967).

4 APPENDIX IV—Introduction to Capacitive Sensors, more on SDC types

The first use of capacitors for sensing mechanical displacements was probably about 1910. In 1920, Cavendish Professor Whiddington, at the University of Leeds, reported his work on a very sensitive displacement sensor of capacitive type [1]. It was a sensor in which the measured observable caused gap spacing change in a single capacitor. In turn, this change altered the frequency of an oscillator circuit; which was compared against a reference oscillator. By counting beats between the two oscillators, the sensitivity of Whiddington's detector was of the order of 1 Angstrom. Although very sensitive, his detector did not have a large dynamic range.

Single capacitor detectors, which rely on gap spacing variation in a specific application, have also been used in more recent experiments [2]. They have been the primary tool for doing harmonic generation studies using ultrasound—a means for measuring anharmonicity of the interatomic potential of solids, such as copper.

In recent years, effectiveness of capacitive sensors in general has been made greater by causing differential change of two capacitors in a single transducer [3]. A popular configuration for their use has been that of a bridge. Because a bridge comprises four components, two of the elements besides the capacitor pair were inactive ones in these cases. A common bridge configuration has been that for which the inactive components derive from the center tapped secondary winding of a ratio transformer. The oscillator drive to the bridge was supplied through this transformer, and the output was directed to a synchronous detector. The synchronous detector— also called a "lock-in" amplifier, was first used extensively for scientific work by Robert Dicke [4]. Much of the pioneering work with bridges of this type was done by R. V. Jones [5].

In 1987, in response to needs borne of the Strategic Defense Initiative (Kirtland Air Force Base, AFOSR program) a new rotary sensor was developed. This invention is one for which the number of active capacitors per transducer was increased from two to four, resulting in a sensor that is doubly (or symmetric) differential [6]. When configured in its most common form, this detector is an example of a "full-bridge". Although full-bridges have been commonly used in resistive sensors, such as the strain gauge; the capacitive counterpart was not utilized before 1987.

With the increased symmetry came improvements in both sensitivity and dynamic range. In the years following 1987, the technology was generalized from rotation to include linear displacement and bending or bowing. This broad new class of symmetric differential capacitive (SDC) sensors permits the modernization of some important old instruments. For example they've allowed the Cavendish balance to become computerized [7]; and in general, they permit the detection of very small changes in physical dimensions. An extensometer, based on one SDC sensor type, can perform measurements in the range from 10 nm to 1 mm in a wire that is several cm's in length. A tiltmeter, based on an array of SDC sensors, can see floor tilt < 10 nrad. Consequently, a variety of fascinating physics can thus be studied in the border region between quantum physics on the one hand, and classical physics on the other. Much of the foundation for these mesodynamic mechanical system studies was laid more than 70 years ago. Their meaningful pursuit had to await improvements in instrumentation, such as the SDC invention.

In section 3.5 is described an SDC sensor which functions on the basis of area change (Fig. 7). Other SDC sensor types depend on gap spacing change, and can be very sensitive. For example, one based on a bowing diaphragm can detect pressure variations as small as 0.01 Pa, or 1 part in 10 million of atmospheric pressure. It is similar to conventional pressure transducers in its use of a diaphragm , but its improved sensitivity results from its increased electrical symmetry. This particular sensor was fabricated with ordinary copper clad printed circuit board, and the gap spacing between the PC board electrodes and the aluminized mylar diaphragm is large by conventional standards. It is estimated that the sensitivity could be increased two orders of magnitude by going to a smaller gap and using greater care in construction. Nevertheless, even the inexpensive present version permits many novel applications, including some obvious medical ones.
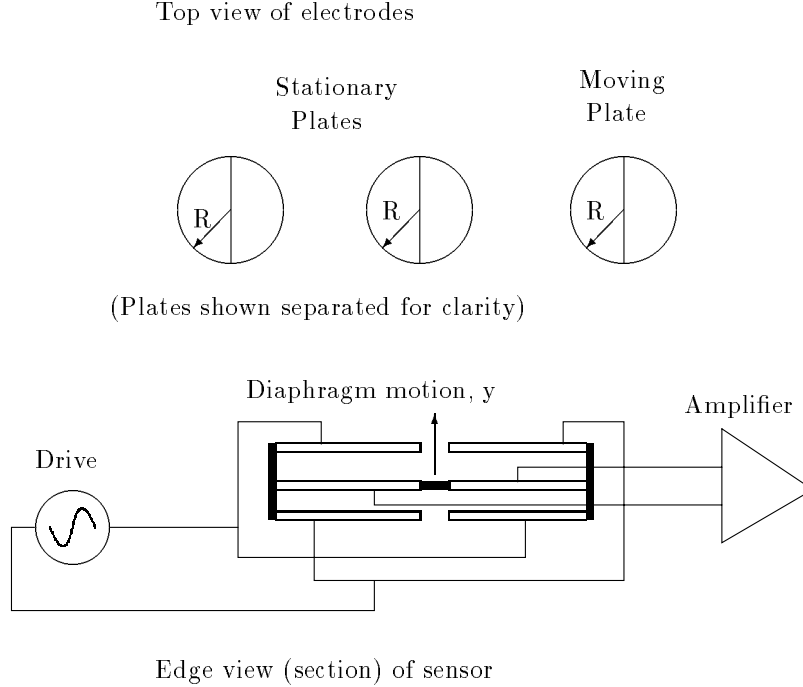
Top view of electrodes

Stationary
Plates

Moving
Plate

(Plates shown separated for clarity)

Diaphragm motion, y

Amplifier

Drive

Edge view (section) of sensor

Figure 3: Illustration of an SDC Pressure Sensor.

4.1 SDC Pressure Sensor

Figure 3 illustrates the SDC pressure sensor, which has been used for a variety of novel demonstrations, as well as quantitative experiments [8]. Details of construction, electronics for its use, and one technique for calibration are all provided in the indicated reference. For clarity in Fig. 3, the electrodes are shown separated in the top view.

As compared to a conventional differential capacitive sensor of the same size, the SDC device has twice the sensitivity—if the stray capacitance, C_s, between the sensor and the instrumentation amplifier is negligible. This can be shown by comparing the equivalent circuits of the two. Each of the four capacitors in the singly differential case has a value (at null of the bridge) given by $C_0 = \epsilon_0 A / d$ where ϵ_0 is the permittivity(essentially that of free space when operating with an air gap), and A is the area of either electrode 1 or 2 (πR^2). In the SDC case (doubly differential), the electrode area is $A/2$. There are 6 electrodes, each having area $A/2$; but four of the six are cross connected, resulting in only 4 total equipotentials. All expressions for capacitance ignore fringe (edge) effects.

The singly differential sensor requires the addition of two capacitors, each of magnitude, C_0, to complete the bridge. The active capacitors are C_1' and C_2', which respond to diaphragm motion, y, in the following manner.

$$C_1' = \frac{\epsilon_0 A}{d} \left(1 + \frac{y}{d} \right) \tag{58}$$

$$C_2' = \frac{\epsilon_0 A}{d} \left(1 - \frac{y}{d} \right) \tag{59}$$

(Note: These are rough approximations, because the diaphragm experiences bowing rather than a uniform displacement, y, across its diameter.)

All four capacitors of the bridge change in the symmetric differential case. The two independent values of capacitance (opposite components of the bridge being equal) are given by

$$C_1 \ = \ \frac{\epsilon_0 \ A}{2d} \ (1 \ + \ \frac{y}{d} \ ) \tag{60}$$

$$C_2 \ = \ \frac{\epsilon_0 \ A}{2d} \ (1 \ - \ \frac{y}{d} \ ) \tag{61}$$

By using the Thevenin equivalent circuit, looking back into the bridge from the amplifier, the following output voltage ratios are obtained:

$$\frac{V_{0h}}{V_i} \ = \ \frac{y}{2d} \ \frac{C_0}{C_0 \ + \ C_s} \tag{62}$$

$$\frac{V_{0f}}{V_i} \ = \ \frac{y}{d} \ \frac{\frac{C_0}{2}}{\frac{C_0}{2} \ + \ C_s} \tag{63}$$

where the subscript, h (for half-bridge), applies to the singly differential case; and f (for full-bridge), applies to the SDC case. V_i is the magnitude of the voltage driving either bridge. Thus it can be seen that the symmetric differential sensor is always more sensitive than the conventional (singly) differential sensor. If the stray capacitance is ignorable, then it is more sensitive by a factor of 2. If the stray becomes very large compared to C_0, then the two have equal (low) sensitivity.

It should be noted that the final result of the analysis just presented applies to every SDC sensor type.

References

[1] R. Whiddington, "The Ultra-micrometer; an application of the Thermionic Valve to the measurement of very small distances", Phil. Mag. 40, 634 (1920).

[2] The early experiments of this type were conducted by Will Gauster; c.f., W. B. Gauster and M. A. Breazeale, Rev. Sci. Instrum. *37*, 1544 (1966). A number of other scientific papers have been published, such as: E. Meeks, R. Peters, and R. Arnold, "Capacitance microphones for measurement of ultrasonic properties of solids", Rev. Sci. Instrum. *42*, 1446 (1971).

[3] See, for example, R. Pallas-Areny and J. Webster, *Sensors and Signal Conditioning* Wiley, New York (1991).

[4] Robert Dicke, "Microwave radiometer", Rev. Sci. Instrum. *17*, 268 (1946).

[5] R. V. Jones and J. C. S. Richards, "The design and some applications of sensitive capacitance micrometers", J. Phys. E: Sci. Instrum. *6*, 589-600 (1973).

[6] R. Peters, "Linear rotary differential capacitance transducer", Rev. Sci. Instrum. *60*, 2789-2793 (1989).

[7] This balance, and a variety of other instruments using SDC sensors, is sold by TEL-Atomic Inc. of Jackson, Michigan.

[8] R. Peters, "Symmetric differential capacitive pressure sensor", Rev. Sci. Instrum. *64* (8), 2256-2261 (1993).

5 APPENDIX V— Mesodynamics

5.1 Preface

Texas Tech University has been the site of research on physical properties of materials, mostly those involving defect structures of metals that are responsible for anelasticity. Several of the TEL-Atomic PAPA instruments have been used in this research. Creep is an example of anelasticity, in which Hooke's law is not obeyed; rather the stress-strain curve displays hysteresis. It has been most thoroughly documented in its continuous classical forms in the well-known book by Zener. Although anelasticity is a phenomenon which was first recognized in the 19th century by some of the great men of physics, it is not a field that has been seriously considered by physicists in recent years. Part of the reason is because anelastic phenomena could not be adequately modeled before the development of the computer, because of the nonlinear equations which regulate virtually every part of it.

The word "chaos" is not as appropriate to the description of anelasticity as is the word "complexity", which includes chaos as a subset. The complexity features show up most dramatically in the mesodynamic realm ["mesodynamic" being a term recommended in 1988 by Brian Davies (University of Texas at El Paso) to describe the nature of this research]. The word "meso" means "in the middle"; and indeed, many of the observed phenomena are in the "gray area" between classical dynamics and quantum dynamics.

The pendulum (in a variety of configurations) has been a primary apparatus for this research (along with a sensitive extensometer). The pendulum is an example of a mechanical system, and before chaos it was naively considered to be a simple one. It has been said of the pendulum that until we fully understand it we can't really hope to adequately understand physics. Because the pendulum is the paradigm of nonlinear physics (contrasted with the simple harmonic oscillator as the paradigm for linear systems) such an understanding is not automatic and certainly not trivial. It might appear, at first glance, that all which remains is simply "tying up loose ends". Nothing could be further from the truth when it comes to mechanical systems. For example, a rigid pendulum can behave reasonably close to theory, only if the "rigid" parts are elastic—or if anelastic, in ways that are subject to the calculus (invented by Newton to solve the two-body problem). In reality, at low levels there are no such systems. About 70 years ago two French physicists (Portevin and Le Chatelier (PLC) discovered an effect which has been virtually lost to the physics community. In the PLC effect, alloys under stress experience sudden increases in length which violate the fundamental theorem of calculus. Moreover, the length can change in a quasi- periodic manner. More recent work of a mesoscopic nature has shown that virtually all metals (pure or alloyed) and probably most polymers can demonstrate this and other peculiar effects. These peculiar properties are the result of cooperative phenomena, the nature of which is presently unknown—a kind of "musical chairs" in which atoms are influencing and being influenced by defects.

That the PLC effect was practically lost, even though published in an esteemed journal, was possibly due in part to timing. It was discovered at the same time as quantum mechanics was being developed. Whereas our now conventional reductionist approach to physics fit quantum mechanics perfectly, it is a disaster when it comes to complexity. Even if the PLC effect had received wide acclaim in the 1920's, there probably would have been unsatisfactory progress, because of the need for a computer.

One area where conventional wisdom concerning the pendulum has been severely lacking is in the area of resonant drive of a dissipative system. If there are no environmental disturbances (such as microseisms) to start the motion, then there is a drive amplitude threshold below which sustained coherent pendulum motion cannot be realized, at least for long period pendula. Moreover, the free decay of such a pendulum, in the mesodynamic realm, is characterized by transitions between metastable states. These probably derive from features of the internal friction of materials that relate in some way to the PLC effect. The defect structure of the metals comprising the support materials is clearly not static.

5.2 Introduction

From the time of Bardeen's work which resulted in the transistor, the physics community has understood that defects can determine the electrical properties of a semiconductor. Much less appreciated by

the community is that defects, of a different kind, can regulate the mechanical properties of a solid, especially metals. The materials science community has recognized the critical importance of defects, such as dislocations, for many years. By empirical means, metallurgists have learned much about defect structures in relationship to the strength of materials. Nevertheless, theoretical advances in this realm have been painfully slow. One famous physicist who did much to advance the cause in the 1940's was Neville Mott, who with his associates provided signficant theoretical insight into the importance of dislocations (c.f. page 21 of Rotherham's book[1]. Another theorist whose contributions have been very significant is F. R. N. Nabarro. In his *Theory of Crystal Dislocations*, Dover, New York (1967 and 87) he even notes the following on page 794: "It is likely that all muscular movement depends ultimately on the propagation of dislocations."

It's unfortunate that other outstanding theorists have not been similarly motivated. Mott may not have become involved either, were it not for the British needs of World War II. Interestingly, much of MIT's greatness derives from radar research during the same time frame and for similar reasons.

Historically, textbooks of solid state physics have paid little attention to dislocations; or they have had a chapter dealing with them that was added somewhat in afterthought, as a type of appendix. One of the author's mentors, Vic Pare' of Oak Ridge National Laboratory, provided him a marvelous means of understanding their importance by a simple analogy. Imagine that you want to translate a large rug on a floor, and that the coefficient of friction between the rug and the floor is significant. With great force, you could pull on an end and accomplish the move. The work required can be far less, however, by forming a "wave" at one end and "walking" it to the other end. Compared to the first method, the primary final difference is that this "dislocation" method takes longer and the work required is less. This point is important, as we shall see later. The fundamental processes to describe mesoanelastic complexity are characterized by very much lower frequencies than excitations with which we are accustomed. Finally, concerning this analogy with the rug, it should be noted that the creep of metals is very slow compared with atomic processes. The characteristic time for conversion from primary to secondary creep can be typically minutes to years. For those unfamiliar with creep and the language developed to describe it, the following is provided from Rotherham (ibid, p.9), "...primary creep is the work hardening stage in which the resistance of the material to creep is being built up by virtue of its own deformation; the secondary creep is a state of balance between work-hardening and thermal softening; and tertiary creep is a period of imminent fracture in which the material is in process of failing either through intercrystalline cracking or some other cause." [Note particularly the reference to thermal softening—the process is never a static one at the atomic or grain level.]

A number of historical curiosities are worth noting in relationship to defects in metals. An important effect is that which was discovered by Portevin and Le Chatelier in 1923[2]. The materials science community sometimes refers to the oscillatory behaviour as one of "serrated yielding".

A phenomenon which may be related to the PLC effect has been known also for many years, but apparently only as a curiosity. Even a common Chemistry and Physics Handbook [3] speaks of the phenomenon known by the German term, zinngeschrei ("tin cries") [4]. If an ingot of pure tin is deformed, audible sounds are emitted. Hofmann speaks of this phenomenon, which has been long known with metals cast into blocks; he attributes the acoustic signature to internal friction between crystal surfaces. Unlike the PLC effect, involving alloys; this phenomenon is known to occur in pure specimens of both tin and indium. There's also another important difference. The frequency of a zinngeschrei acoustic signature is much higher than that associated with the PLC effect. The PLC phenomenon is more in the category of "infrasound". What then, is the primary difference between the PLC effect and zinngeschrei? Perhaps they are related phenomena, both involving dynamics which is likely to be best understood at the mesoscopic level. The processes certainly involve defects, particularly intergrain boundaries in some unknown way. That such a fundamental cooperative phenomenonhas been mainly forgotten is quite surprising.

Another curiosity is as follows. One of the founders of dislocation theory proposed an interesting

---

[1] Creep of Metals, Institute of Physics, London (1951)

[2] A. Portevin and M. Le Chatelier, "Tensile tests of alloys undergoing transformation", Comptes Rendus Acad. Sci. 176, 507 (1923).

[3] CRC Press, 53rd ed., p. B-16 and B-34 (1972)

[4] K. A. Hofmann, Anorganische Chemie, Friedrich Vieweg Sohn Braunsch Weig, p.609 (1956)

but mostly unknown concept. Taylor speculated that dislocation lattices should exist, since the Burgers vector can alternate in sign [5]. Correspondingly, one might envision an ordering which is in some ways similar to the Madelung description of an alkali halide crystal. Seitz's old book on the Physics of Metals [6] is one of the few that refers to postulated dislocation arrays. One of the more dramatic consequences of such an array is long range ordering. Unlike an atom, where the potential falls off rapidly with distance; that of a dislocation line falls off slowly. Thus there are potentially dramatic consequences in the mesoscopic realm. In particular, consider the following. The natural consequence of an ideal (harmonic) lattice at finite temperature is normal mode vibrations, which when quantized, give rise to phonons. If dislocation lattices exist, then they should be characterized by excitations of a presently unknown character, but presumably with at least remote similarites to phonons. Unlike phonons, these excitations are fundamentally nonlinear, and thus given to chaos and complexity. An important question concerns their coherence time. At first thought, one might speculate that there's no way such an excitation could persist. However, at least one theory has shown that the kink in a dislocation line obeys the sine-Gordon equation and thus is the medium for a soliton[7].

A number of well known 19th century scientists were intrigued with the physics of anelasticity. (In the present context, as in all others discussed by the author, the definition of anelasticity is according to the seminal work of Zener[8]. For example, J. C. Maxwell, J. H. Poynting and J. J. Thomson were quite familiar with the fact that metals manifest deviations from perfect elastic behavior, even at small stress levels. (ibid, page 126). Although interest by physicists in the subject has been rare in the 20th century; nevertheless, it occupied the thoughts of one of the greatest men of the previous generation. In his lecture series on physics, Richard Feynman[9]. duplicated in its entirety a reprint of Lawrence Bragg's paper dealing with bubble rafts, titled "A dynamical model of a crystal structure"[10]. Feynman was obviously fascinated, as were Bragg and Nye, with the dynamics (during return to equilibrium) of the defects present in two dimensional bubble structures after vigorous stirring. It is also significant that Fig.7 of this original paper involves a dislocation lattice. In fact Bragg and Nye refer (following Taylor) to the positive, negative, positive (reading from left to right) parallel dislocations. Moreover, dislocation lattices have been positively identified in metals.

In the last 10 years there has been considerable attention within the actuator community to the properties of shape memory alloys. In the world of microelectromechanical systems (MEMS), the unique properties of SMA materials are thought by many to hold special promise[11]. This "wire with a memory" was invented many years ago. It changes crystal structure (austenitic to martensitic) about 20 C above room temperature. Because of the large free volume associated with the phase transition, its memory features are quite impressive. It should be noted, however, that memory is a characteristic of anelasticity, even in pure materials that don't undergo transformations. In fact, memory is the basis for hysteresis. This point was recognized and clearly stated by a South American physicist who wrote an article on the subject in Physics Today in the early 1950's.

Part of the present premise—cooperative phenomena of mesodynamics is not yet widely accepted. The term, mesodynamics, combines the words "mesoscopic" and "dynamics". It involves measurements on samples, such as wires, whose length is in centimeters; but for which changes in length are typically nanometers. Thus the strains involved are an order of magnitude, or more, smaller than previous work which involved "microstrains". For purpose of dialogue which follows, the term "nanostrain" may sometimes be used. Because mesodynamics involves anelasticity; and because the processes are fundamentally complex, the the term "mesoanelastic complexity"[12] was originated.

The curiosities mentioned earlier concerning anelasticity, along with nearly a decade of experimental observations, have prompted two predictions—first, that the indicated curiosities are part of a (yet to

[5] G. Taylor, Proc. R. Soc. 145, 362 (1934)

[6] The Physics of Metals, McGraw Hill, New York, p.92 (1943)

[7] A. Pawelek and M. Jaworski, J. Appl. Phys. 64, 119 (1988)

[8] Elasticity and Anelasticity of Metals, Chicago Press (1948).

[9] R. Feynman, Lectures on Physics, Addison Wesley, Vol. II, p.30-10, 1964

[10] L. Bragg and J. F. Nye, Proc. Royal Soc. of London, 190, p.474 (1947)

[11] (One may purchase an inexpensive titanium-nickel (titinol) wire for demonstration purposes from DaMert Co., Dept. T, 2476 Verna Ct., San Leandro, CA 94577)

[12] "Experimental evidence for a new frontier—mesoanelastic complexity", Nonlinear Phenomena in Complex Systems Seminar, Belarus (1994)

be developed) new frontier (footnote 12). In this frontier, involving mesoanelastic complexity, there are sometimes excitations that become large enough to manifest themselves in the macro-domain. For example, this is true of the PLC effect and zinngeschrei. (Meso is here defined as length changes less than 1 μm.

The second prediction has to do with the following. Just as mechanical excitations known as phonons determine many of the physical properties of ideal materials; so likewise there must be fundamental collective excitations within the defect structures of real materials. In keeping with physics tradition, it is recommended that these excitations be referred to as **krazons**. The reasoning behind this recommendation is as follows. Traditionally (except with high energy exceptions, such as quarks), the root for a name has been the Greek word describing the related process. Thus phonon comes from phonos for sound. In the present case, krazo is the Greek word for "cry", the suffix of zinngeschrei. *The krazon is defined as follows: "A cooperative excitation in a meso-complex system, which is fundamental to internal friction, and which arises from slowly varying macro-forcing. At larger scales it manifests itself in zinngeschrei (tin "cries") and in the Portevin Le Chatelier effect."*

Prior to giving some experimental evidence for krazons, the following food for thought is provided. When anelasticity figures into the lengthening of a metal wire, such as by creep; hysteresis (memory) is inevitable. When the length change is large enough to be a macro-size increase, the process of atomic rearrangement is normally thought to be hideously complicated. At the meso-level however (nanostrains), it appears that some of the processes may be amenable to theoretical treatment. In particular, consider the fact that an increase in wire length must have an accompanying increase in surface to volume ratio. An important question is, how do atoms move from the bulk to the surface of the wire to accomplish this change? Experiments suggest that this is not a random process; but rather one in which krazons are the vehicle for accomplishing the task. One possibility is that a single atomic layer of atoms is being transferred from the bulk to the surface of a wire during length increase. Observations on silver wires are in keeping with this hypothesis. Curiously, the wire can be stimulated by a mechanical impulse, under some conditions, to execute the reverse process and become shorter. The memory features of anelasticity make these quantal length changes more readily acceptable, since demonstrations of stimulated creep recovery are usually met with great surprise, and even skepticism.

It should be noted that the change being discussed is not instantaneous. Atoms are not likely to spontaneously jump to the surface everywhere along the whole length of the wire. Rather, the more likely scenario is one of an atomic ledge that moves, atomic spacing at a time (by jumps), from one end of the wire to the other. Because of dislocations, the total stress in the wire need not be large (remember the analogy with the rug). As noted earlier, softening through thermal effects (even at room temperature) is known to be important; so there is an inherent mechanism to facilitate transitions between the enormous collection of metastable states that characterize the anelasticity[13]. Moreover, the postulated moving ledge is likely a spiral, as suggested by Mike Marder. Such a model looks less preposterous when one considers the manner in which wires are "drawn". To reduce the diameter of a wire, it is typically drawn through successively smaller diameter dies. Thus the material may be preconditioned toward the "jumps" described.

An important feature of the postulated krazon is its nominal lifetime, from milliseconds to seconds. The author has observed coherent (phase preserving, reasonably monochromatic) excitations whose lifetimes can be several seconds. As compared to atomic scale femtoseconds, such long lived excitations are "older than the age of the universe".

It is surprising the extent to which mechanical system properties have been ignored by the physics community. G. Venkataraman has spoken to this issue and admonished physicists to get involved in what he felt should become an important new field[14].

Prior to recent work, the PLC effect was apparently observed only in alloys in the macroscopic realm. Numerous studies of plasticity and creep have shown that yield is generally not continuous, but exhibits discontinuous serrations. These discontinuous steps are now known to continue down to the mesoscopic scale, even in pure materials. Additionally, in this realm the systems can be manipulated, through temperature and-or mechanical stress, into states of complexity. For example, the length of metallic

---

[13] T. Erber, S. Guralnick, and S. Michels, "Hysteresis and fatigue", Annals of Phys. 224 (2), 157 (1993)

[14] "Fluctuations and mechanical relaxation", in Mechanical and thermal behaviour of metallic materials, Proc. Enrico Fermi Int. School of Phys. LXXXII, eds. G. Caglioti and A. Milone (North-Holland, Amsterdam, 1982), pp. 278-414.

wires will sometimes fluctuate between two states, similar in some respects to the two-well macroscopic mechanical oscillator.

Studies of meso-mechanical complexity have not been easy because of hysteresis and associated problems of reproducibility. The resulting need for statistical interpretation of data collected over long time intervals in slowly varying systems has been a great challenge. It has taken more than five years to develop sufficient confidence to assert that the observations are as claimed, and not the result of instrument anomalies such as electronic artifacts. There have been some fortuitous exceptions to the more common case of nonreproducibility, however. For example, at elevated temperatures, some pure polycrystalline metal wires show reproducible temperature hysteresis in their length fluctuations, suggesting a thermally stimulated transition between two distinct states, one or both of which must involve some unknown long range order[15]. It has been speculated that these states might result from dislocation lattices, previously mentioned. Moreover, the excitation responsible for the transitions could be a **krazon**. This is based on the observation that the time required for the transition is slow, in keeping with anelastic phenomena in general.

5.3 Example of complexity—Bistability

One of the most interesting cases of complex meso-mechanical behavior is that which occurs when a wire fluctuates between two states. Paired states have been observed in samples which change both torsionally and in length. Examples of both kinds were reported at the 1994 Belarus conference (see footnote 12). One case involved the position of the boom in a Cavendish balance. Fluctuations persisted for about 30 s during a 7 min record. The peak to peak maximum of the fluctuations was about 750 μrad. The fiber of this balance was a Tungsten wire about 7 cm long with a circular cross sectional diameter of 25 μm. Anelastic changes of the boom position are common in such an instrument, particularly after a new torsion wire is installed. Thus it is expected that these effects have been a significant contributor to the poor precision with which "G" has been established over the years. With optical detection schemes used by most previous investigators, fluctuations and mean position changes were not so readily discerned.

An example of spontaneous fluctuations involving length change was also provided at this conference. The sample was a silver wire (99.9 percent pure) of 0.127 mm diameter, 18 cm long. Prior to the record presented, the then virgin sample had been conditioned by "shakedown", which will be explained later. The maximum of the spontaneous changes was approximately 2 μm, corresponding to the smallest observed separation of states for the sample. It was noted there that the values of "2" and "4" might not be coincidental. There was evidence for the length preferring to change in multiples of 2 μm, possibly due to the transfer of a single atomic layer $4x10^{14}$ atoms to and from the surface of the wire. It is speculated that this could be a krazon phenomenon, perhaps in terms of a "barber-pole" ledge moving along the wire.

There was some question in earlier studies as to whether (i) temperature fluctuations, (ii) convective air flows, or (iii) electronics instabilities might be responsible for the variations. One can reasonably rule out (i) and (ii) , because the measurements were performed at room temperature in a nearly isothermal basement laboratory. Concerning (iii), it is unlikely that the electronics should vary in a manner consistent with the observations.

5.4 Shakedown

Cycling a metal around ever larger hysteresis loops is a process in which the range of elastic behaviour can be increased through work-hardening. For metals of high initial plasticity, this hardening occurs largely through the pinning and entanglement of dislocations. The sample will have experienced "shakedown" for a given stress level, once cycling back and forth between zero and the level shows insignificant anelastic response. One of the most recent (exhaustive) treatments of the phenomenon reports on the studies of Erber and co-workers (c.f. footnote 13).

Instead of using, as Erber et al, a continuously variable stress to cycle through the hysteresis loops, the present work accomplished shakedown by the following means. Starting with a small weight on the extensometer pan, the wire was allowed to creep in the primary phase, without hammer blows. [It

---

[15]R. Peters, "Fluctuations in the length of wires", Phys. Lett. A 174, 216 (1993)

is not unusual, during primary creep, for μm size PLC jumps to occur in pure metals, such as lead.] After the creep rate had decreased significantly, a heavier weight was placed on the pan. Additionally, the creep could be dramatically accelerated by impulsive blows to the table. The final length of a wire experiencing creep at a fixed stress appears to be independent, within certain limits, of whether or not the wire is influenced by impulsive blows. It can be forced much more rapidly to the endpoint, however, by means of blows.

5.5 Stimulated Creep Recovery

It has been known for years that micro-creep recovery can be facilitated by means of alternating stress[16]. Recent work shows that impulsive blows may be even more efficient at stimulating creep recovery. It appears that the sample responds selectively, from the broad spectrum of the blow, to that frequency which is most effective in stimulating recovery. It should be noted that recovery, because of memory features, after long periods of creep, can persist for much longer than most people would guess. This is especially true for ductile metals such as indium and tin. After creeping for one hour, evidence for recovery also persists for about one hour. The recovery rate is about an order of magnitude smaller, however. (Probably this statement is meaningful only for nanostrains.)

5.6 Critical Fluctuations

It was the concept of "evolution toward a critical state" that prompted studies involving impulsive blows. Because avalanches of snow can be triggered by dynamite explosions, it was reasoned that a "delta-function" type hammer blow could trigger length changes in a wire under tension. This method for stimulating PLC-like jumps has proven to be extremely effective.

The dramatic response to sharp blows suggests that there is probably a frequency range of mechanical excitation to which the jumps are sensitive. A preliminary test of this hypothesis was performed by driving the weighted extensometer pan through a weak spring, connected to a loudspeaker which was powered by a frequency and voltage adjustable oscillator. Nonlinear phenomena were observed, in which jumps toward longer length could be readily stimulated by starting at a frequency of about 100 Hz and then slowly scanning to below 10 Hz. [By contrast, jumps were not observed when scanning in the opposite direction from low to high.] Transitions occurred most often (perhaps always) at frequencies for which transverse standing waves were established in the wire. The frequency of the drive was found to be much more important than the amplitude, as long as it was above a critical threshold, whose value was not measured. These experiments suggest the possibility that PLC jumps, in general, are an avalanche phenomenon of SOC origin that may be triggered by environmental vibrations.

Previous experiments showed spontaneous fluctuations, evidently between two states. Not all attempts to obtain bistability have been successful, however. This illustrates the difficulty of studies of this type. It is not generally possible to follow a simple "recipe" and obtain reproducible results. What was found with creep of indium was a transient period of large fluctuations (about 1 min total duration) of essentially 1/f type, during creep. Apparently this resulted timewise in the vicinity of the transition from primary to secondary creep–after first loading with a 10 g mass, removing, stabilizing and then putting on a 5 g mass.

One has to question whether electronics could be responsible for variations that have been seen. Of course the general lack of reproducibility makes it difficult to establish confidence that they are not artifacts. Because this has been a bigger issue in the past, means were sought for increasing the signal to noise ratio in the measurements. Thus the earliest work, in which the threshold of sensitivity was about 100 nm has been lowered to about 10 nm (for SNR = 1). The primary means for this improvement was by adding a transformer. One can also detect still smaller signals by means of signal averaging techniques. For example, by retaining only the low frequency components of the FFT and then doing the inverse transform, an effective low pass filtering operation can be performed. A window (such as Hamming) should be used in the process. For the present work, it was not necessary to extend below 10 nm, because the fluctuations of interest (way above electronics) are in the tenths of μm's.

---

[16]A. J. Kennedy, Processes of Creep and Fatigue in Metals, Wiley New York, p. 293 (1963).

5.7 Long-Periodic Behaviour

There is strong evidence from a variety of experiments that metallic wires exhibit mesoscopic coherent oscillations in length. This is a truly remarkable result when one considers that their coherence time can be more than five cycles, with periods up to several seconds. Compared to the characteristic time for atomic processes, the lifetime of a single krazon can be "greater than the age of the universe". An established confidence in their existence was not possible on the basis of studies at elevated temperatures alone, because of factors such as unknown temperature stability and air convection. Several independent experiments support their existence. There was a case with the low frequency mesodynamic pendulum in which oscillation was maintained in its lowest "harmonic state" (period of 30 s) for the better part of an hour. At the time the APL paper was composed, the best guess for the source of motion of the "undriven" pendulum was low level seismic activity. Subsequent experiments suggest that an alternative, and possibly preferred, explanation is the mechanism described in the following section.

5.8 Parametric Mechanical Oscillations

The following observations appear to be well established: (i) micro-creep can be recovered, as noted earlier, by means of an applied periodic stress (or even sharp stimuli that apparently excite vibratory modes), (ii) prior conditioning of a wire, such as work hardening, can place it in non-equilibrium (metastable) states, and (iii) the strain energy of these states is released slowly, which is why pendula with periods longer than 15 s are required to see the interesting features of complexity. These observations provide the following basis for explaining sustained mechanical oscillations, in the absence of external drive, of a pendulum held together by wires. Oscillation of the pendulum provides a source of stress modulation in the wires. Micro-creep recovery in the wires is accomplished through unknown stimulation processes, at the proper time in a cycle of periodic stress, so as to maintain oscillation. A simple analogy is that of a ball on a string in which the string is shortened, in proper phase, at twice the frequency of oscillation.

Sustained oscillations have also been seen in a pendulum other than that described in APL. This long period pendulum was built in the following way, by modifying an old-fashioned chemical analytic pan (mass) balance. The boom was severed just to one side of the agate knife edge (primary) of the balance, and another knife edge bearing (secondary) was inserted where the boom had been broken (see Fig. 30, section 5.10). To hold the system together, which was now flexible at the secondary knife edge; vertical outrigger posts were added to each of the two ends of the boom. A wire sample of $\approx$ 18 cm length in tension between the posts was all that kept the boom from collapsing about the secondary knife edge. This system is a physical pendulum whose period, and thus sensitivity, is adjustable in a well known manner–by altering the vertical position of a small mass that moves on the indicating pointer. The attractive feature of this system is its ability to simultaneously accomplish two important tasks with ease; i.e., provide (i) low level periodic stress in the sample, its magnitude being determined by the amplitude of oscillation, and (ii) a controllable mean stress in the wire by the size of the matched weights placed on the pans of the balance.

A number of interesting experiments have been performed with this apparatus, which is enclosed by glass to minimize the effects of air currents. For example, in one experiment an inductor coaxial with the wire sample was added to provide a controlled magnetic field. Complex phenomena of peculiar type were seen in a variety of different samples. Especially interesting was the response when the polarization state of an iron wire was altered by means of a solenoid coaxial with the sample. Not only were polarization changes in iron observed to give rise to fluctuations, but the internal friction could also be dramatically altered.

The most interesting experiment of all using this apparatus was one which supports the previously postulated notion of parametric mechanical oscillation by stimulated creep recovery. A 0.2 mm dia. copper wire was irradiated for 45 min with a heat lamp to establish a non-equilibrium state. No attempt was made to estimate the wire temperature for its specified 40 cm distance from the 250 W infrared lamp. During irradiation, and also during record collection, the mean stress in the wire was constant. The record was initiated at the time of lamp turn-off, and oscillation was observed that persisted for 135 min. It is believed that the motion could not be sustained in a quasi-periodic manner for such a

long period, on the basis of thermal gradients in the system. The time required for the system to return essentially to room temperature was much less than this. The mean position could be altered as the result of thermal gradients; however, significant oscillations were not observed with certain other wire types.

Evidence for oscillation of a similar type but through a different excitation means was also recently discovered using a heavy Cu wire in the extensometer. A fixed stress of $4x10^7 N/m^2$ was maintained on the sample (dia. 0.32 mm). The initial strain rate was large at 1.4 ppm/s and was a dominant feature. Also noticeable, however (above electronics noise) was a high frequency component (or components) which was found to "wax and wane" with a variable frequency around 10 seconds. This modulation was strikingly similar to the earlier phenomenon at much lower frequency involving a Cu wire in the analytic balance pendulum. Usually, the high frequency part is made more visible by removing the secular term (creep) and increasing the gain by a factor of 10. Where does this signal come from? Is it a krazon? It was found to result from two vibration modes of the instrument, but the source of excitation was clearly the creep itself.

5.9   Preliminary Experiments in Vacuum

About 1993, some preliminary experiments were conducted in vacuum. The pressure attained with a roughing pump was about 100 μm of Hg, which is poor, but which should be low enough to remove significant convective disturbances to the extensometer when the wire sample is heated. The reason for raising the temperature of the sample is obvious. It has been long known that annealing can cause dramatic differences in the physical properties of metals. Concerning the previously mentioned fluctuation studies at elevated temperatures, there remains uncertainty as to whether the long periodic features of those experiments were truly intrinsic to the sample as opposed to resulting from periodic convective flows. The reproducible parts of the experiment (fluctuation hysteresis) are not thought to be influenced by convection. It could be, however, that the air plays an undetermined role in the magnitude of the hysteresis. For example, silver was found to fluctuate at unbelievably large levels (100's of μm's) in the air furnace as the temperature came to within about 100 degrees of the melting point. Currently it is believed that this unusual phenomenon may be associated with the complex oxide states of the surface. Certainly, additional experiments with silver are called for, particularly in vacuum.

An obvious sample material for use at elevated temperatures in vacuum is the common alloy of nickel and chromium. Because of its high resistivity, nichrome wire (which is used in heater elements) can be easily elevated in temperature by passing a current through it. An unusual length response was found in a NiCr wire of 80 μm dia., 25 cm long, after being heated with a current of 100 ma for just a few seconds. The record was taken after the wire had returned essentially to equilibrium. This was rapid because of its small thermal inertia, even though the primary heat transfer is via radiation. There was a remarkable frequency modulation associated with the resulting disturbance, assumed to be a krazon. In some respects it looks like a wave packet, but not the typical quantum mechanics type. In other respects it appears more similar to solitons on the surface of water. It is an excitation which was first seen in an entirely different system--the analytic balance instrument previously mentioned. There the frequency was too high for fine structure to be seen with the strip chart recorder being used (before a computer acquisition system was added). To resolve the packet, the drive to the recorder was modified so that very rapid rotation of the drum recorder (old seismometer type) was possible.

Additionally, some experiments were done with Pd in vacuum. After pumping the system down, the Pd wire was found to exhibit, at room temperature, 1/4 μm oscillations--one mode at 0.57 Hz and the other at 10 Hz. The 0.57 Hz promptly converted to 1.1 Hz (2nd harmonic) and there were later additional modes at 1.33 as well as 12 Hz.

5.10   Metastable States of Mesodynamics

Previously mentioned were the metastable states observed at low levels of a non-driven, low frequency physical pendulum. At large levels, the decay of the pendulum has been described as a type of mechanical Barkhausen effect. It is known from work by Erber's students that the Barkhausen effect is radically different between polycrystalline and single crystal samples. Thus the coupling between mag-

netic domains and grain boundaries is important. At large levels of the pendulum the loss of energy (internal friction), due to grain boundary rearrangement, involves large numbers of variations equivalent to domain "flips". A quantal amount of energy may be associated with the "flip" (called a hysteron, following Erber's suggestion and discussed later). Perhaps the krazon carries integer multiples of the hysteron, whose energy is $10^{-11}J$. Thus at large levels the decay looks relatively smooth, but in the mesodynamic range the number of flips becomes small; so that the decay is through metastable states.

Metastability of a similar type has also been seen in a torsion balance operating in vacuum. The torsion wire (tungsten) was tied at both top and bottom. Two 50 g masses were on the end of a nearly weightless boom; their separation was 38 cm. Undeniable metastable states were present after the amplitude had dropped below about 100 μrad.

5.11   Evidence for Meso-mechanical Quantum dynamics

For many of the observations mentioned, it would seem the best choice of terms to describe them should be ones which include the word "quantum". Physicists are conditioned, however, to believe that quantum phenomena of mechanical type (such as with a pendulum) should not be visible, at least at room temperature. This assumption may not correct, however, for reasons provided in the paragraphs which follow.

Superconductivity and lasing; as examples, are now recognized as macroscopic quantum phenomena[17]. Curiously, use of the term to describe superconductivity is only recent, in spite of our long-time knowledge of the phenomenon. A popular misconception concerning quantum physics is that parameters must be infinitesimal; which clearly is not true of the quantum Hall resistance ($\approx$ 25 kΩ). Such great size is possible because, as Fritz London recognized, macroscopic occupation of a single state can endure in spite of large interactions (fluctuations and-or couplings to the environment). Quoting Bardeen: "If many electrons are involved in a phase-coherent step, the energy involved can be much larger than thermal energy even though the energy per electron is smaller".

Historically, the first observation of any macroscopic quantum phenomenon has probably been characterized by astonishment. For example, von Klitzing says of his discovery of the quantum Hall effect: "It is quite astonishing that it is the total macroscopic conductance of the Hall device which is quantized, rather than some idealized microscopic conductivity."

In virtually every discovery of a quantum phenomenon, experiment has preceded any attempt to try and understand that phenomenon. The theoretical difficulties are extreme because of the nature of many-bodies, and surprises are inevitable. For example Stamp[18] has theoretically predicted large (mesoscopic) quantum entities previously unexpected. He theoretically predicts that large domain walls, containing $> 10^{10}$ spins can behave as quantum objects. Conventional wisdom has said that no more than 10,000 spins could be correlated. He points out that the choice of a relevant macroscopic coordinate from all other degrees of freedom is not trivial.

Concerning the properties of metals, most everyone would agree; that at the macroscopic level, the complexities of creep are bewildering. This is surely one reason why physicists have turned the problem over to engineering, for empirical study. There has been a sense of hopelessness associated with trying to gain understanding. Some, if not most of the macro-problems are indeed hideous; however, it is believed that portions may be tractable in the mesoscopic range.

Recent evidence to support this claim comes from studies performed on nanowires, using a scanning tunneling microscope [J. I, Pascual et al, "Properties of metallic nanowires: from conductance quantization to localization", Science, Vol. 267, 1793, 24 March 1995.] This team has observed conductance quantization attributed to changes in the contact area during elongation of short and thin Au nanowires, about 40 Angstroms long. Especially curious is the fact that the conductance changes in multiples of $2e^2/h = 77.2 \ x \ 10^{-6} \ A/V$. To quote from their paper: "The appearance of room-temperature quantized conductance in the short wires and its persistence ..... are remarkable".

A need exists for modifying our way of thinking, as encouraged by Kataraman. First of all, we need to recognize that almost nothing is known about the manner in which macroscopic energy of plastic

---

[17] J. Bardeen, Phys. Today 43 (12), 25 (1990).

[18] "Quantum dynamics and tunneling of domain walls in ferromagnetic insulators", Phys. Rev. Lett. 66 (21), 2802 (1991).

deformation is converted into heat. Certainly, nonlinear processes are necessary to accomplish the conversion. Only by this means can macroscopic stressing at very low frequencies be transformed into the frequency range of phonons. Theoretically, it might be profitable to think in terms of a quantum (the hysteron) as a vehicle to facilitate the necessary up-conversions in frequency.

The hysteron, as a dissipative counterpart to quantized flux jumps, is a concept which originated with Tom Erber, of Illinois Tech University. He pointed out that the smallest energy change in the pendulum exhibiting metastability was "hilariously" near the ratio of the electron rest energy to the fine structure constant (1.1×10^{-11} J). Whether coincidental or not, this observation led to the subsequent discovery of the thermal hysteresis loop in palladium, having an energy in the same neighborhood. *The hysteron is defined as follows: "A postulated quantum of hysteresis loss involving krazons, which has a value of 1.12 x 10^{-11} J . It is the dissipation counterpart to quantized flux jumps in complex systems.*

Is all of this coincidental, or is a significant new frontier being opened? It is hoped that these observations are sufficiently interesting to spur others to get involved in similar work. To quote Erber, "physicists are dying of thirst without realizing that there's a great body of fresh water all around them".

6 APPENDIX VI— Krazons in the Earth

6.1 Free Earth Vibrations

Free earth vibrations set into motion by large earthquakes have been known since 1961 [1]. During 1990, while doing experiments concerned with gas desorption from solid surfaces, Kwon observed responses of a torsion balance that correlated with the earlier earthquake data. He and Peters have submitted a paper titled "The study of eigenmode types and source nonlinearity in the free earth oscillations" to the Journal of Korea Physics Society (1994). A chapter dealing with the study is also to be found in Kwon's PhD dissertation [2](number V). The abstract of the paper that is under review reads as follows:

"By measuring the changed mean position of a modified balance, we have almost continuously observed long period oscillations of the earth from January to August, 1990. Periods of those vibrations are correlated with more than ten of the known long periods of spheroidal and torsional oscillations of the earth which resulted from large earthquakes. The amplitudes of the fluctuations we have observed are correlated with the lunar synodic period, indicating that they are driven by tidal forces. Also, these fluctuations have some properties of chaotic motion due to nonlinearity of the source."

Because an earthquake is localized (virtually a delta function in space), it's efficiency for exciting global modes of the earth is very poor. This is why the free earth modes have been seen only after large earthquakes (roughly Richter 7 and bigger). Obviously, the best candidate for exciting global modes is a global forcing function— the tidal force. If at a given point in time, the tidal force (at maximum) could be suddenly turned off, then free earth oscillations would result. Conversely, if the earth should experience a rapid internal structural relaxation while being forced by the tides (12 hour periodicity); then this will also result in free earth vibrations. (The relaxation time necessary for triggering of the modes must be short compared to the period of an oscillation.) Studies suggest that low level, short lived eigenmodes are excited by this method sometime during nearly every lunar synodic period. Moreover, these modes may be similar to those which are sometimes triggered, as the result of anelasticity, in metallic wires undergoing periodic stress. Concerning the latter, the following definition of the Krazon is found in Appendix V of the present monograph:

"A cooperative excitation in a meso-complex system, which is fundamental to internal friction, and which arises from slowly varying macro-forcing. At larger scales it manifests itself in zinngeschrei (tin "cries") and in the Portevin Le Chatelier effect (PLC)" [3].

Possibly there are scaling features to these oscillations which transcend size; i.e., similar features may exist between a cm sized wire on the one hand, and the earth on the other. Regardless, neither of the systems obeys Hooke's law; i.e., they are not elastic.

To provide an experimental basis for these claims, some background on geophysical instrumentation is now given.

6.2 Tiltmeters and Angle Measuring Equipment

6.2.1 General Description

The tiltmeter is an instrument whose output is determined by the mass distribution of the earth, since it responds to the local acceleration of gravity, $\mathbf{g}$. Also sometimes called an inclinometer, particularly if its range is large; the response of the instrument is determined by the direction of $\mathbf{g}$ relative to its orientation. The principles of operation can be illustrated with common tools of carpentry. Consider a static plumb-bob, which would constitute a spherical pendulum if the system were dynamic. The plumb-bob orients itself along the direction of $\mathbf{g}$, and thus defines the local vertical. Alternatively, a fluid bubble, contained by a tube, will determine one of the locus of directions, orthogonal to $\mathbf{g}$, which constitute the local "level".

There are two ways in which the output from a tiltmeter can be altered. The first and commonly understood case, is one which occurs when the platform holding the instrument experiences an acceleration, such as by rotation. It can result from either the instrument housing being moved with respect to the ground, or from the ground itself moving. The latter is the basis for earth studies using the horizontal seismometer; which, as a tiltmeter, is sometimes referred to as a "garden-gate" pendulum. In effect, it is a "variable g" pendulum in which $g_{eff} = g \sin\beta$, where β is the angle of the axis with
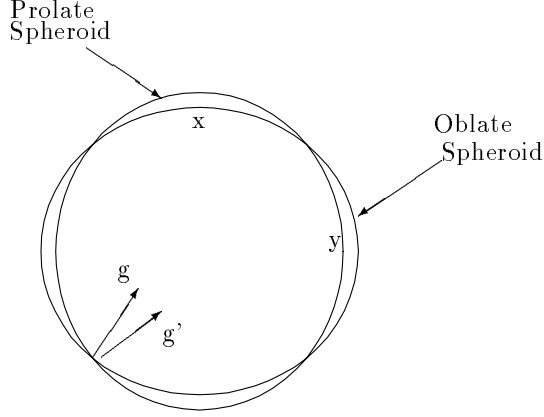
Figure 4: Illustration of the lowest frequency Free Earth Eigenmode.

respect to g . The details of its oscillation, due to a disturbance, are determined by the convolution of the external forcing function with the instrument's response to an impulse (i.e., its Green's function). β is especially important because the period is given by:

$$T = 2\pi\sqrt{\frac{I}{mL\,g\,sin\beta}}$$

where I, m, and L are, for the pendulous element, the moment of inertia, mass, and perpendicular distance from axis to center of gravity (cg) respectively. Unlike the plumb-bob, practical instruments are constrained to one degree of freedom, responding only to the component of acceleration which is perpendicular to the axis-cg plane. Thus a complete description of the disturbance requires two tiltmeters at right angles to each other.

The second type of tiltmeter disturbance requires an instrument of very high resolution. In this case, the acceleration is virtually zero, but the direction of **g** is altered due to a distortion of the earth in which there is a global redistribution of its mass. For example, if properly positioned with a sufficiently sensitive instrument, one should be able to observe changes in the direction of **g** due to free vibrations of the earth. As recognized by geoscientists, these modes are standing waves which could be used as a mathematical basis for describing the various waves generated during earthquakes. They were first observed with strainmeters after large earthquakes. Additionally, however, an early generation of the tilt sensitive pendulum of this monograph (section 5.9) has produced evidence for the previously mentioned 10 spheroidal and torsional free-earth modes excited by tidal forces acting on the rotating anelastic earth. The longest measured period was 54 min, consistent with the lowest order spheroidal eigenmode. This mode is one in which there are prolate to oblate deviations from the geoid, as illustrated in Fig. 4.

The figure corresponds to an intersection of the earth with a plane through its center, and the symmetry axes of the spheroids (through x and y), would but rarely coincide with the earth's spin axis. The orbital ephemerides, particularly of the moon, cause the directions of these axes to change from month to month. The lowest order eigenmode, being spheroidal with azimuthal symmetry, is described in Trefil's treatment using the Legendre function, $P_2(cos\ \theta)$ [4]. Thus the standing wave would be given by

$$r(\theta,t) \ = \ a \ + \ a_2 \ cos \ \omega_2 t \ (3 \ cos^2\theta \ - \ 1 \ ) \tag{64}$$

where a is the earth radius, and a_2 is the amplitude of the mode.

The acceleration of the earth's surface at any point is obtained through differentiation.

$$\frac{d^2 r}{dt^2} \ = \ - \ \omega_2^2 a_2 \ cos \ \omega_2 t \ (3 \ cos^2\theta \ - \ 1 \ ) \tag{65}$$

It can be seen that the maximum possible acceleration occurs at $\theta \ = \ 0 \ or \ \pi$ and has a magnitude of $2 \ \omega_2^2 a_2$. Additionally, the acceleration is zero everywhere on the minor circle given by

$cos\ \theta\ =\ 1/\sqrt{3}\ \rightarrow\ \theta\ =\ 54.74\ deg$. Moreover, the change in direction of the acceleration of gravity for points on this circle is given by

$$\Delta g\ =\ \Delta(\frac{1}{a}\frac{dr}{d\theta})\ =\ 5.652\ a_2/a \tag{66}$$

This corresponds to the difference in direction between g and g' in Fig. 4, which is highly exaggerated for purpose of illustration.

There is some question as to whether Eq. (64) is precisely correct. Trefil's treatment is one which assumes the earth to be a spherical mass of fluid. This disallows the influence of certain moduli and results in an estimate for the period of the lowest mode of 94 min rather than the actual 54 min. Regardless, the fact remains that the mode is a standing wave. As such, there is a locus of points on the surface of the earth which must be nodal points; i.e., their acceleration is zero. Thus there are points on the earth for which there should be tiltmeter response devoid of acceleration.

6.2.2 Angle Measurement

In the past, the most common plane angle measurements have involved visual comparisons against a circularly divided scale. For example, the stator full circle of a student spectrometer would be typically scribed with 720 equally spaced fiducial marks; from which the unknown position of the rotating shaft could be directly read to within 1 min of arc (290 μrad) using an adjacent scale of 30 marks. By viewing through a microscope and interpolating, the practical limiting accuracy of instruments of this type is about 1 sec of arc (4.8 μrad).

Another common instrument, of optical type, has been the precision auto-collimator [5]. It will typically measure to 0.5 μrad over a range of 1000 μrad. It is essentially a telescope which superimposes a movable graduated scale on the image. It requires that an optically flat front surface mirror be attached to the rotating object.

One of the simplest, and most common of all angle measuring techniques is that of the optical lever. It has been employed in many physical instruments, such as the Cavendish balance for measuring the Newtonian gravitational constant, G. In this technique, a collimated beam of visible light, such as from a He-Ne laser, is reflected from a front surface mirror attached to the rotating object. The angle change of the reflected beam (twice the amount of mechanical rotation) is determined using the definition of angle in radians; i.e., the ratio of subtended circular arc to the corresponding radius. An overly idealized analysis would suggest that there should be no limit to the resolving power of this instrument, if the path length following reflection could be extended without limit. In actuality, it is very difficult to make measurements to better than 0.1 μrad because of (i) beam divergence, and (ii) increased susceptibility to environmental vibrations at larger path length. Moreover, it is not trivial to generate good permanent records with an optical lever.

A means for overcoming many of the difficulties of the conventional optical lever is to employ interferometric techniques. The first person to do this appears to have been R. V. Jones [6]. Even though "optical lever" appears in the title of his paper, the key to the instrument's great sensitivity is its use of a coarse grating, pictured in Fig. 1 of Jones' paper. In this paper, the coarse gratings, which are traditionally labeled Ronchi rulings among optical personnel, are referred to as grids. It is a great oversight that Ronchi's name is not mentioned, since it is a Ronchi grating interferometer that is described in the Jones' paper. Lest it appear that these statements be too critical of Jones, it should be noted that far too few people have heard of this great instrumentalist (for which the "ch" in his name is pronounced as a "k"). [The editor of Applied Optics had the following comment concerning Ronchi's paper: "...published...to bring this important and interesting technique to the attention of a wider audience."]

It was Texas Tech University associate professor emeritus of physics, Preston Gott, who apprised me in 1987 of the work of this great physicist. He demonstrated Ronchi's grating interferometer with an ordinary white light incandescent bulb. Normally, we think that interferometers require monochromatic light, but not so with this Ronchi system. The bulb was placed at the center of curvature of a long focal length mirror, and a Ronchi ruling was put between them, just in front of the bulb, along with a shield so that one looks only at the light returned from the mirror. (This setup is reminiscent of the Foucault knife edge test for optics; however, because of the coarse grating, it is orders of magnitude more sensitive.)

With this simple system, Preston showed how wavefront distortions can be readily seen in a 10 m optical path by simply raising the temperature of the air at a point in that path by means of one's hand. When the hand is replaced with a soldering iron, the changes in index of refraction give the appearance of a "boiling caldron". Anyone who has ever seen this incredible demonstration would have little difficulty believing the sensitivity claims reported in paper [6].

Ultimately, the credit for any advances in interferometry have to belong, at least in part, to Albert Michelson. An instrument based directly on his famous interferometer was built by Larry Mertz[8], and it has a resolution better than 1×10^{-10} rad with a dynamic range in excess of 200 dB. This impressive level of performance would have been impossible without modern electronics, including the computer.

In their original form, all of the aforementioned angle measuring instruments have required that the data be read and recorded by an individual. The collection of data sets of sufficient size for good statistical confidence was a gruelling task in which the possibility for human errors was significant. This has naturally led to the development of instruments which are suitable for automation. Among early versions, the unknown angle was converted to an appropriate electrical signal by means of (i) resistance change using a calibrated slidewire, (ii) phase change between balanced ac inductive circuits such as the selsyn (synchro/resolver) system, and (iii) change in capacitance or inductance which can alter a bridge circuit or the frequency of an oscillator.

For small angles, where the arc length can be reasonably approximated by the associated chord length, one of the most popular sensors has been the linear variable differential transformer (LVDT). The LVDT has even been modified to measure rotation by means of a cardioid shaped rotor, but the performance of the resulting angle sensor is poor compared to the latest capacitive types. All of these inherently analog instruments have been largely replaced in recent years by digital devices, of which the optical encoder is the most common. The increasing presence of digital systems for information processing and display, particularly the advent of the personal computer, has made these digital sensors very attractive. Nevertheless, for some applications they have serious shortcomings that should not be overlooked [9].

CAPACITIVE SENSORS

As mechanical displacement sensors, capacitive devices have a number of advantages: (i) insignificant loading with no direct mechanical contact, (ii) high stability and reproducibility, and (iii) ease of manufacture resulting in low costs. As compared to inductive sensors, they have been less employed, but that is expected to change due to recently introduced technologies. Their greatest assets had to await electronic developments that could deal effectively with problems that derive from high output reactance and sensitivity to stray capacitance. Prior to amplifiers such as integrated circuit types which use the field effect transistor, it was difficult to exploit their advantages. For an idealized system, one solution to the problem of high output reactance would be to increase the frequency of the oscillator supply; however, real systems derive limited benefit from increased frequency because of stray capacitance effects. Both these and edge effects become less significant for sensors of increased symmetry, such as the new full-bridge or symmetric differential capacitive (SDC) transducers [10]. Additionally, sensitivity is greater by a factor of 2 compared to the half-bridge (traditional) sensor with the same electrode area. Viewed in relationship to the general importance of symmetry in physics, these results should not be surprising. What is a matter of surprise is how long it has taken for their discovery.

The SDC sensor strengths are realized when supported by an instrumentation amplifier and a phase sensitive detector (PSD = lock-in amplifier), which takes advantage of the π shift in phase of the output as the bridge voltage passes through zero. In addition to the outstanding linearity that is thus achieved, these packages are characterized by an outstanding signal to noise ratio, since the vast majority of electronic noise is not correlated with the reference (drive source) input to the PSD. Finally, it should be noted that they can be down-scaled in size without severe penalties, because of an "invariance to scaling" property of their output. This can provide a dramatic improvement in vibration isolation, and additionally it makes them attractive candidates for inclusion in micro-electro-mechanical systems [11].

COMPACT CAPACITIVE TILTMETER

Shown in Fig. 29 of part I of this monograph is an instrument designed for measuring small tilts [12]. In some respects it is similar to the Wood-Anderson torsion seismometer [13]; except that in the present instrument the rotor center of gravity is much closer to the torsion fiber. Thus it can be made sensitive to tilt but insensitive to linear acceleration. Using torsion and gravity in opposition, it is an

instrument having no friction due to bearings (hinges); and it is not severely hampered by internal friction, if material for the torsion fiber is properly selected. The period is mechanically adjustable, tending toward ∞, as $\beta \rightarrow \beta_c$ the point of instability. Sensitivity is proportional to the square of the period, and thus operation near β_c yields a dramatic mechanical amplification of any small tilt, γ, perpendicular to the axis defining β. In practice, it is difficult to operate with periods greater than 30 s because of instabilities that derive from (i) differences in thermal expansion coefficients of components, and (ii) mechanical creep which, although small, can be very important near the critical point.

Studies performed with instruments that are similar to the one described have clearly demonstrated that friction is simultaneously the single most important factor and also the least understood feature of such instruments. Without mechanical amplification, discontinuous phenomena of complex character, related to the Portevin Le Chatelier effect, mask the majority of low-level processes that would otherwise be interesting candidates for study. In the very low-level regime, mesoanelastic complexity frequently dominates the nonlinear dynamics of mechanical oscillation. It has been known for centuries that defects largely regulate the material properties of solids in the macro-regime. Likewise, they are of critical importance to meso-properties, especially as influenced by surfaces. Apparently because of this complexity, common tiltmeters are unable to observe the hypothesized tidal force excited free earth vibrations. This could be due to their purposely large damping (usually near critical), since the only evidence for their existence was from an evacuated instrument of high Q for which the case pressure was $\approx 10^{-6}$ $Torr$.

Rotor motion in the tiltmeter is detected most effectively with a full-bridge capacitive detector array, such as illustrated in Fig. 10 of part I of this monograph. The overall system (tilt) sensitivity is ≈ 1 $nrad$ with a dynamic range $> 150dB$, and its low frequency performance has typically been limited by electronics stability. The output is periodic for large angles, being sawtooth with small "rounding" where the slope changes, due to capacitive edge effects.

Because the output is periodic, performance could be further improved by a combination of digital and analog electronics support. Unlike encoders, where resolution is determined by the number of counts per unit angle, such a device could have much greater resolution–by both counting and then performing an analog measurement between counts. The resolution could be very large because of the steep slope of the voltage vs angle characteristic in the linear regions.

The use of arrays is attractive for another reason–overall size reduction. There is great advantage in mechanical compactness, because the frequencies of undesirable mechanical modes can then be shifted farther from noises of the environment. This provides an increased immunity to noise as compared to larger instruments, just as was noted with scanning tunneling microscopes subsequent to their size reduction. Not only does this increase the signal to noise ratio of the instrument, but there can be improvements in user friendliness and versatility as well.

References

[1] H. Benioff, F. Press, and S. Smith, Journal of Geophysical Research 66, 605 (1961).

[2] M. H. Kwon, "Refinements of a new balance for measuring small force changes", p. 71, PhD Dissertation, Texas Tech University (1990).

[3] A. Portevin and F. Le Chatelier, "Tensile tests of alloys undergoing transformation", Comptes Rendus Acad. Sci. **176**, 507 (1923).

[4] J. S. Trefil, *Introduction to the Physics of Fluids and Solids*, Pergamon Press, N.Y., p 110 (1975).

[5] *Methods of Experimental Physics*, Vol 1, Classical Methods, ed. Estermann, 56 (1959).

[6] R. V. Jones, "Some developments and applications of the optical lever", J. Scientific Instr. 38, 37 (1961).

[7] Vasco Ronchi, "Forty years of history of a grating interferometer", Applied Optics *3*, no. 4, p. 437 (1964).

[8] L. N. Mertz, "Interferometric angle encoder", Rev. Sci. Instrum. **62** (5), 1356-1360 (1991).

[9] R. Pallas-Areny and J. Webster, *Sensors and Signal Conditioning*, Wiley, New York (1991).

[10] R. Peters, "Capacitive angle sensor with infinite range", Rev. Sci. Instrum. **64** (3), 810-813 (1993).

[11] L. O'Connor, "Mems: microelectromechanical systems", Mech. Engr. **114** (2), 40 (1992).

[12] R. Peters, "Mechanically adjustable balance and sensitive tiltmeter", Meas. Sci. Technol. **1**, 1131 (1990).

[13] T. Teng, "Seismic instrumentation", *Methods of Experimental Physics*, Vol. 24 part B, GEO-PHYSICS Field Measurements, 55 (1987).

7   APPENDIX VII—Dimension

It has been noted that strange attractors are fractal and possess self similarity, meaning invariance under a change of scale. We need to have at least a rough idea of what is meant by these terms. The easiest dimension to understand conceptually is that which is called the capacity dimension.

7.1   Capacity Dimension

Consider first a one dimensional figure—a line of length, L . Consider *covering* this line with N short segments, each of length, ϵ . The number of segments required depends on the size of L and ϵ as follows

$$N \; = \; L \; / \; \epsilon \tag{67}$$

Similarly, if a two dimensional figure, $L \; x \; L$ were to be covered by squares, $\epsilon \; x \; \epsilon$, then they would have to number

$$N \; = \; L^2 \; / \; \epsilon^2 \tag{68}$$

Thus we conclude that the number of pieces, for a system of dimension, d , must obey

$$N \; = \; L^d \; / \; \epsilon^d \tag{69}$$

so that the dimension is obtained in general, by taking the logarithm, as

$$
\begin{aligned}
d \; &= \; \frac{Log \; N}{Log \; L \; - \; Log \; \epsilon} \\
&= \; \frac{Log \; N}{Log \; L \; + \; Log \; \frac{1}{\epsilon}}
\end{aligned}
\tag{70}
$$

Since the $Log \; L$ term in the denominator becomes insignificant as ϵ gets very small, we arrive at the following definition of the capacity dimension

$$d_c \; = \; \lim_{\epsilon \to 0} \frac{Log \; N(\epsilon)}{Log \; \frac{1}{\epsilon}} \tag{71}$$

	N	ϵ
————————————————	1	1
———————— ————————	2	1/3
—— —— —— ——	4	1/9
– – – – – – – –	8	1/27

Figure 5: The first three steps in generating the Cantor Set.

7.1.1 Cantor Set

Classic examples of two simple fractal systems are the Cantor set and the Koch curve. These are described in detail by Benoit Mandelbrot— *The Fractal Geometry of Nature*, Freeman, New York (1977, 1982, 1983).

Fig. (5) illustrates the first several steps in generating the Cantor set. The construction begins with a line segment of length 1. It is subdivided into three equal sections and the middle one is removed, leaving a total of two segments. The process is continued for each of the remaining segments, ad infinitum.

In the limit, the total length of the set approaches zero; however, the dimension is between 0 and 1. This can be seen as follows. On the right in Fig. (5) are values of N and ϵ at each step of the subdivision. After n steps, it can be seen that

$$N = 2^n$$
$$\epsilon = 1/3^n \tag{72}$$

Thus from Eq. (71), the capacity dimension is seen to be

$$\textbf{Cantor Set}: \quad d_c = \frac{\text{Log } 2}{\text{Log } 3} = 0.631 \tag{73}$$

7.1.2 Correlation Dimension

Experimentally, it is sometimes the case that only one state variable is available. Thus we construct a pseudo-phase-space, or embedding space, using time-delayed measurements. The dimension of the space can be estimated using the correlation function, $C(r)$, which is defined as

$$C(r) = \frac{1}{N^2} \sum_i \sum_j H(\ r\ -\ |x_i\ -\ x_j|) \tag{74}$$

where the Heaviside function $H(s) = 1\ if\ s > 0$ and $H(s) = 0\ if\ s < 0$. To obtain the dimension of the system

$$d = \lim_{r \to 0} \frac{Log\ C(r)}{Log\ r} \tag{75}$$

In practice, one obtains the dimension as the slope of the (ideally) straight line in a plot of $Log\ C(r)\ vs\ Log(r)$. The correlation dimension is also useful in cases where there is more than a single variable available. We illustrate the technique with an example from the research of Brian McCuistian, concerned with the failure of dielectrics subjected to large electric fields. Fig. 6 is from the computer algorithm which he developed to model the trees (in 2-dimensions), that approximate failures that he has observed experimentally. The experimental system is referred to as a point-plane geometry; i.e., a needle embedded in a dielectric slab on top of an electrode plane. (This work by McCuistian and
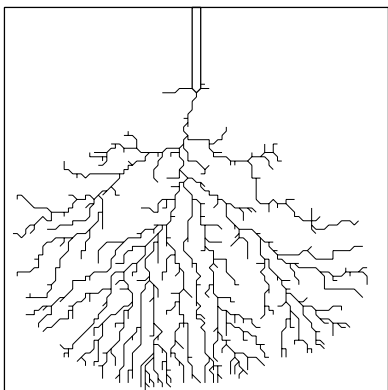
Figure 6: Simulated dielectric breakdown tree.
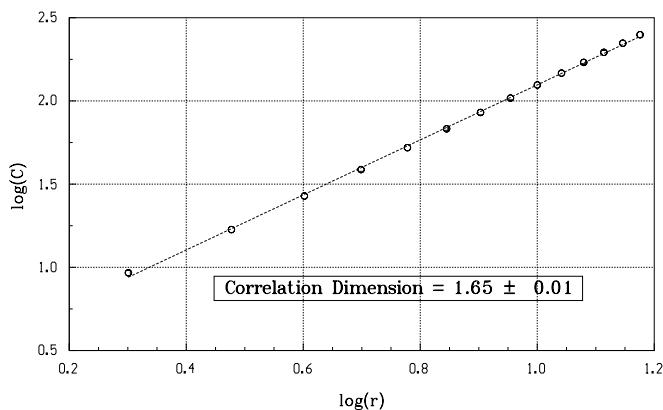
Figure 7: Graph for calculating the correlation dimension of the Fig. 6 tree.

Hatfield will be published at some time in the future in one of the IEEE journals dealing with electrical insulation.)

Because of the branchings, this structure is obviously fractal, with a dimension between 1 and 2. Brian calculated the correlation dimension according to the method described above, in which he obtained the log-log graph of Fig. 7. Note the very well defined straight line, which has a slope of 1.65, corresponding to the dimension of his tree. The uncertainty in this value is only 0.01, which is small compared to most cases.

Brian wrote his own algorithm for estimating the correlation dimension (tailored to his specific case). Sprott's "Chaos Data Analyzer" package contains an algorithm for computing the dimension when working with a single variable. (Physics Academic Software: TASL, Box 8202, North Carolina State University, Raleigh, NC 27695-8202.)

Appendix V mentions work by Kwon concerning free earth vibrations. It was found that mode switching, which appears chaotic, has a fractal dimension of 5.6 ± 0.3. As Kwon noted, this does not prove that oscillations of the earth are chaotic. It may be the result of tight coupling between a large number of eigenmodes. Whichever (or both) of the two cases is true, the result is certainly due to nonlinearity. The magnitude of the fractal, at 5.6, is one of the bigger numbers usually encountered.

36

Index